J. Math. Computer Sci., 35 (2024), 388–410

Online: ISSN 2008-949X

Journal of Mathematics and Computer Science

Journal Homepage: www.isr-publications.com/jmcs

Stochastic modeling of malware propagation on reduced scale-free topology-based wireless sensor networks: dynamics, resilience, and countermeasures

Cheikhna B'ayir[a,*], Mohamed Essouifi[a], Youness El Ansari[b], Abdelfattah Achahbar[a], Jamal El Khamkhami[a]

[a]Condensed matter physics laboratory, Department of physics, Faculty of sciences, Abdelmalek Essaâdi University, B.P 2121, Tétouan, Morocco.

[b]IRF-SIC Laboratory, Faculty of Sciences, Ibn Zohr University, Agadir, 80000, Morocco.

Abstract

In this paper, we present an approach to model the stochastic spread of malware within a wireless sensor network (WSN). The network is characterized as a reduced scale-free topology, exhibiting just two average degrees. Our work delves into the realm of stochastic epidemic modeling building upon its deterministic counterpart [19]. We leverage two distinct methodologies, namely the discrete-time Markov chain (DTMC) and the Stochastic Differential Equation (SDE) techniques, to explore the temporal dynamics of our proposed model. Our investigation extends to analyzing how various model parameters influence infection within WSNs. Through Monte Carlo simulations and the Euler-Maruyama discretization scheme, we validate the credibility of our two stochastic models by demonstrating their congruences and their fluctuations around the deterministic solution reliant on nonlinear coupled ordinary differential equations (ODEs). This comparison is guided for the best understanding of the stochastic fluctuations effect in the dynamics of the spread of malware in WSNs. Our findings offer valuable insights, indicating that the network exhibits enhanced resilience against network failures and more balanced energy consumption when specific countermeasures are implemented. This probabilistic framework proves both meticulous and systematic, providing a profound understanding of the intricate randomness inherent in the behavioral patterns of malware within WSNs.

Keywords: Stochastic spread of malware, wireless sensor network, reduced scale-free topology, discrete time Markov chain, stochastic differential equation, Monte Carlo simulations, Euler-Maruyama discretization scheme.

2020 MSC: 60G99, 92-04, 60H10.

1. Introduction

Wireless Sensor Networks (WSNs) comprise sensor nodes or motes wirelessly connected. They employ sensors that monitor physical conditions, generating relevant sensory data. Each node integrates essential components, including a processing unit, memory, communication module, and power supply, with constrained processing, data collection, and transmission capabilities. Sensor nodes transmit data to base stations or sinks upon detecting events of interest. Sinks communicate with end-users through

*Corresponding author
Email address: cheikh.med1992@outloook.fr (Cheikhna B'ayir)

doi: 10.22436/jmcs.035.04.02

Received: 2023-11-26 *Revised:* 2023-12-20 *Accepted:* 2024-05-05

various channels, including direct connections, the Internet, or wireless links. Despite inherent limitations, WSNs find applications in diverse fields like security tracking, intrusion detection, environmental monitoring, traffic management, and positioning systems, positioning them at the forefront of research interest. However, key challenges in WSN research revolve around energy resource depletion and node vulnerability to potential attacks. A viral attack leading to sensor node failure could disrupt the network structure, causing fragmentation, reduced coverage, or complete paralysis.

In advancing WSN research for practical applications, efforts focus on two key directions. Researchers aim to enhance the security, robustness, and efficiency of WSNs by (i) establishing stable, efficient topologies resistant to attacks [8, 16, 17, 31, 44, 47, 48]; and (ii) modeling malicious attacks using a macroscopic epidemic approach in both homogeneous [1, 21–23, 30, 42] and heterogeneous networks [9, 20, 24, 32, 40, 45]. This dual pursuit reinforces WSN's effectiveness in real-world applications by ensuring reliable monitoring and data transmission to the sink. In the track of the first research direction, Wang et al. [44] developed the Arbitrary Weights-based Scale-Free topology control (AWSF) algorithm to minimize transmission delay and increase robustness in WSNs. These arbitrary weights are random real numbers following a negative power law probability distribution. Ye et al. [47] studied a scale-free routing protocol and algorithm in WSNs, including routing reliability, network bandwidth usage, energy reserving, and life cycle. This algorithm could significantly reduce the redundancies of the datagram transferred in the WSN and thus improve the life cycle of WSN. To balance the connectivity and energy consumption in the network, Jian et al. [17] proposed an energy-aware BA (EABA) model for WSNs, which takes into consideration both node degree and residual energy in preferential attachment that has been introduced by Barabási and Albert [6, 7]. Jiang et al. [18] suggested a local-area and energy-efficient (LAEE) evolution model for wireless sensor networks. The model proved to have better tolerance against energy depletion or random failure than other non-scale-free WSN topologies. Qiu et al. [31] designed an algorithm called ROSE for enhancing the robustness of scale-free networks against malicious attacks, and compared it with two previous robustness-enhancing algorithms [8, 16]. The comparison shows better robustness enhancement results and consumes less computation time. Duan et al. [10] introduced a cluster-structured evolution model of WSNs that combines characteristics of the scale-free network and small-world network, that is, the scale-free effect focuses on the enhancement of network survivability and small-world effect attempts to shorten the transmission paths within the network. They concluded that these features make the network maintain superior error tolerance (in the case of a random attack) and have better energy efficiency and intrusion tolerance (in an intended attack).

These studies collectively reveal that homogeneous networks (fall within the second research direction) inadequately reflect the topology of WSNs, especially in terms of reliability and robustness when faced with viral attacks causing the failure of one or more nodes. Consequently, there has been a shift in focus toward heterogeneous networks, with particular emphasis on scale-free configurations. This strategic pivot, which also aligns with the second research area, has emerged as a direct response to address the identified inadequacies associated with homogeneous networks. Indeed, Rey et al. [32] improved a homogeneous cellular automated into an individual-based model where particular features of the router and sink nodes have been used. More than one isolated outbreak has been exhibited in this model, and the first one appeared before the outbreaks in the previous models. Shen et al. [40] proposed a heterogeneous model, in which they took into account the communication connectivity of heterogeneous sensor nodes and the characteristics of the self-hiding malware and dysfunctional sensor nodes. They derived the malware spread threshold and compared their simulation results with the conventional SIS and SIR models. They showed the effectiveness of the model from the perspective of achieving equilibrium. Muthukrishnan et al. [24] studied a malware trace-patch mixed propagation model over WSNs, taking into account both the topological structure of the network and its geometrical shape. They used an optimal control strategy to minimize the number of infected nodes and the budget. They numerically illustrated that the proposed method achieves the minimum cumulative cost within the bound. Based on the three ideas (i) the inner sensors are often highly linked compared to the outer ones which in turn are highly connected compared to the gateway nodes; (ii) the robustness of the network in case of power depletion or malicious attacks depends largely on the non-failure of motes with higher connectivity; (iii) the WSN is considered to be a reduced scale-free network [14, 46], Keshri et al. [19] developed an epidemic model of WSN to explore the significance of the higher connectivity motes in maintaining the overall robustness of a WSN during a malicious attack.

Our study delves into the intricacies of stochastic epidemic modeling of the preceding deterministic counterpart [19]. We utilize two distinctive methodologies, namely the discrete-time Markov chain (DTMC) and stochastic differential equation (SDE) techniques, to explore the potential temporal dynamics of the proposed model. Our work further encompasses the stochastic simulation of how diverse model parameters exert influence on infection dynamics within WSNs.

The remainder of this paper is organized as follows. In the next Section 2, we discuss the limitations of relevant studies that have addressed the second research area, and we detail our model's proposition. In Section 3, we delineate the distinctions between DTMC and SDE methods in modeling stochastic systems. Then, we provide a discussion following a detailed description and formulation of our proposed DTMC and SDE models. In Section 4, we simulate both models and present countermeasures for WSNs. We conclude with a comprehensive summary and appendices, offering additional insights into the methodology and findings.

2. Limits of the existing models-our proposal

The references cited above that concerning the modeling of the spread of malware on WSNs have focused on deterministic models. They only forecast a single and average outcome of a given set of coupled nonlinear ordinary differential equations (ODEs) with absolute certainty. Actually, by taking into account the stochastic behavior of the malware spread, deterministic models fail to describe and understand their realistic dynamics. As is well known [2, 14, 15, 26, 33], stochastic models, whether those that based on Markov chain Monte Carlo (MCMC) techniques or those that uses continuous time stochastic differential equations (SDEs), are the best alternative choices for achieving this goal. Unfortunately, there are few achievements that approached the topic of the spread of malware over WSNs using stochastic epidemiological models, or studies that compare the results of both deterministic and stochastic approaches in this field. For instance, Zhong et al. [51] established a heterogeneous model to describe and control the dynamics behavior of malware spread in WSNs. They use an aperiodically intermittent controller driven by white noise, which has striking advantages of lower cost and more flexible control strategy. In the work cited above [24], the authors only used the GEMFsim algorithm which is available on popular scientific programming platforms [38, 39] to estimate each node's probability distribution over the state in the network. Then, they plotted a single realization of an average of 100 simulations of the SITPS model on a random network, and they compared it with the outcome of the deterministic one. This is nothing but a solution of the nonlinear ODEs which are based on the first-order mean-field approximation. To investigate the offensive worm dynamics in WSNs, Zhang et al. [50] analyzed an e-SITR model by incorporating the Holling type-IV and the white noise stochastic perturbations. The noise has been introduced to understand whether the dynamical behavior of the deterministic model is strong for such a sort of stochasticity by exploring the asymptotic steadiness conduct of the equilibrium point, contrasting the outcomes and those acquired for the Ito stochastic differential framework. Nwokoye et al. [28] proposed an epidemic model to study the effects of both concurrent worm and virus categories on WSNs. They extended the deterministic model by incorporating external noise to change the deterministic nature of the original model and permit stochastic analyses for random factors such as temperature and physical obstructions. Both models admit the same equilibria, and the stochastic one fluctuates around its average states.

It is true that in some stochastic models cited above, node-level heterogeneity has been taken into consideration, but ideas of dividing network nodes into two distinct classes (hubs and lowly linked nodes), and then treating each class separately by a different epidemiological model have been neglected. Thus, these references have just limited to studying an epidemiological model consisting of only one chain of compartments. However, in WSNs, by the fact that the outer sensors generally have fewer links as compared to the inner ones which in turn have less degree compared to the gateway sensor motes, we propose to investigate a stochastic model which takes into account these assumptions.

Inspired with the works in the field of the prevalence of infectious diseases in population biology [2–4, 25, 29, 34], and those in the field of the propagation of computer viruses over networks [5, 12, 14, 15], we develop the DTMC and the SDE models to stochastically explore the impact of reduced scale-free network parameters on the spread of malware upon a wireless sensor network-both stochastic epidemic models derived from their deterministic counterpart [19]. The authors of this work [19] took advantage of the idea of reduced scale-free network [46] to study the local stability of an epidemic model established on a wireless sensor network.

In a first stage, we use the mean of random variables to analyze the discrete-time stochastic processes of two sub-chains of the Susceptible-Exposed-Infected-Recovered-Susceptible and Susceptible-Exposed-Infected-Recovered (SEIRS-SEIR) model. The aim is to randomly predict the spread of malicious attacks on a wireless sensor network and compare the obtained findings to those arising from the deterministic model [19]. Furthermore, To enhance network robustness during power outages or malicious attacks, it is crucial to minimize failures in high-connectivity nodes, as emphasized in the previous work [19]. However, given that both high-connectivity and low-connectivity nodes are influenced by model parameters, our research herein delves into comprehensively assessing the impact of these parameters on the overall fraction of infections. Besides, some measures have been suggested to make the entire network more resilient to network failure and to maintain balanced energy costs. In the discrete-time stochastic computation, the model is assumed to be a Markov chain, in which the probability of each subsequent state is conditionally independent of all previous states and depends solely on the probability of the current state. It is also supposed that the time step is small enough that during that period, at most two events and only one change in each node state occur. Indeed, a single node within the RSFN cannot make concurrent transitions. This means it cannot, for instance, jump from the exposed state to the infected state and back to the exposed state within the same time step Δt. Additionally, two different nodes in the RSFN cannot move simultaneously from an exposed state to an infected state during the time step Δt. Thus, our proposed discrete-time stochastic model is formulated as a Markov chain by considering two conditionally interrelated sub-chains, SEIRS and SEIR, with a constant population size for both, (see Figure 1). The transition probabilities for the two sub-chains, The transition probabilities for the two sub-chains, as well as the conditional probabilities linking them, are computed using the same method as described by Essouifi and Achahbar [14, 15] (see Appendix), and the resulting difference equation that characterizes the model's temporal evolution is presented.

In a second stage, two parameters of the deterministic model are supposed to be subject to environmental noise, namely, the probability per unit of time that a k_2-degree node leaves the sensor field (denoted μ), and the probability per unit time that k_2-degree recovered nodes again become susceptible because of the temporary immunity (denoted δ) are perturbed by a type of noise that may represent the environmental random variability. The choice of this perturbation is justified throughout the paper and existence, unicity and globality of the obtained SDE is proved. By using a well known discretization scheme, the paths of the three random variables corresponding to the fractions of exposed, infected and recovered sensor nodes for the SDE are plotted in superposition with their paths using the DTMC model and the deterministic model. The objective of this simulation is to measure the degree of similarity between the two methods of perturbation, and analyze the effect of perturbing the parameters μ and δ in the dynamic of the SDE. Therefore, this paper can be considered as paving the way for studying more realistic and more complex stochastic epidemiological models, in which the network can be divided into three or four different classes depending on the degree of nodes.

3. DTMC and SDE models: description, formulation and discussion

We emphasize that both methods (DTMC and SDE) are used to model systems with inherent randomness, but they provide different mathematical frameworks for studying these systems, with key distinctions in time continuity, state space, and modeling approach. In the DTMC method, time progresses in discrete steps, and the space state is also discrete. For instance, consider a system that can be in state $|m\rangle$ at time t and transition to state $|n\rangle$ at time $t+\Delta t$, where $t = 0, \Delta t, 2\Delta t, 3\Delta t, \ldots$. The transition between states occurs with certain probabilities, and these probabilities adhere to the Markov property, signifying that the future state depends solely on the current state and not on the sequence of events leading to the current state. The evolution of the system is described by transition probabilities $p_{|n\rangle,|m\rangle}(t+\Delta t, t) = P\left\{|n\rangle \,\middle|\, |m\rangle\right\}$. Conversely, the SDE method considers both time and space states as continuous. SDE incorporates continuous stochastic processes, often modeled by a Wiener process. It provides a framework to describe the continuous evolution of a system by specifying the rate of change of a variable to time, including a stochastic differential term. This differential term introduces randomness, capturing the inherent uncertainty in the system's dynamics: $dX_t = a(X_t, t)dt + b(X_t, t)dW_t$, where dW_t is the stochastic differential term. This equation expresses how the random variable X_t evolves over time, influenced by both deterministic ($a(X_t, t)dt$) and stochastic ($b(X_t, t)dW_t$) components.

3.1. DTMC model

We assume that the network owns N_1 nodes (sensor nodes or motes) of degree k_1, N_2 nodes of degree k_2 and no nodes of any other degree, where $k_1 \gg k_2$. N_1, N_2, k_1, and k_2 are unvaried in time. Thus, the network owns exactly $N = N_1 + N_2$ nodes whatever the time t. For $j = 1, 2$, let $S_j(t)$ (respectively $E_j(t)$, $I_j(t)$, and $R_j(t)$) denote the discrete random variable for the average number of k_j-degree susceptible (respectively exposed, infectious, recovered) t. Let $S(t)$ (respectively $E(t)$, $I(t)$, and $R(t)$) denote the discrete random variable for the average number of susceptible (respectively exposed, infectious, recovered) nodes at time t such that: $S(t) = S_1(t) + S_2(t)$, $E(t) = E_1(t) + E_2(t)$, $I(t) = I_1(t) + I_2(t)$, $R(t) = R_1(t) + R_2(t)$. For $j = 1, 2$, let $s_j(t) = \frac{S_j(t)}{N_j}$ (respectively $e_j(t) = \frac{E_j(t)}{N_j}$, $i_j(t) = \frac{I_j(t)}{N_j}$), $r_j(t) = \frac{R_j(t)}{N_j}$) denote the discrete random variable for the average relative density of k_j-degree susceptible (respectively exposed, infectious, recovered) nodes at time t. Let $s(t) = \frac{S(t)}{N}$ (respectively $e(t) = \frac{E(t)}{N}$, $i(t) = \frac{I(t)}{N}$, $r(t) = \frac{R(t)}{N}$) denote the discrete random variable for the average density of susceptible (respectively exposed, infectious, recovered) nodes at time t.

The schematic representation of deterministic model in Fig. 1 is equivalent to the following coupled nonlinear ODEs, with satisfying initial conditions $0 \leqslant S_1(0), E_1(0), I_1(0), R_1(0) \leqslant N_1$, and $0 \leqslant S_2(0), E_2(0), I_2(0), R_2(0) \leqslant N_2$. The conditions are chosen such that $S_1(t) + E_1(t) + I_1(t) + R_1(t) = N_1$ and $S_2(t) + E_2(t) + I_2(t) + R_2(t) = N_2$, where $E_1(t)$, $I_1(t)$, $R_1(t)$ (resp. $E_2(t)$, $I_2(t)$, $R_2(t)$ denote the average number of k_1-degree exposed, infectious, recovered) (resp. k_2-degree exposed, infectious, recovered) nodes at time t:

$$\begin{cases} \dfrac{dE_1(t)}{dt} = k_1\beta\left(N_1 - E_1(t) - I_1(t) - R_1(t)\right)\Theta(I_1(t), I_2(t)) - \alpha E_1(t), \\ \dfrac{dI_1(t)}{dt} = \alpha E_1(t) - \gamma I_1(t), \\ \dfrac{dR_1(t)}{dt} = \gamma I_1(t) - \delta R_1(t), \\ \dfrac{dE_2(t)}{dt} = k_2\beta\left(N_2 - E_2(t) - I_2(t) - R_2(t)\right)\Theta(I_1(t), I_2(t)) - \alpha E_2(t) - \mu E_2(t), \\ \dfrac{dI_2(t)}{dt} = \eta_2 N_2 + \alpha E_2(t) - \gamma I_2(t) - \mu I_2(t), \\ \dfrac{dR_2(t)}{dt} = \gamma I_2(t) - \mu R_2(t). \end{cases} \tag{3.1}$$

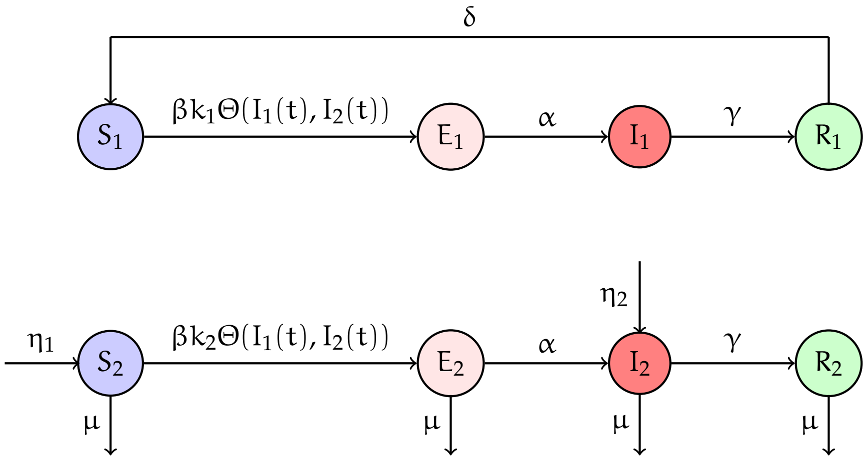

Figure 1: Schematic diagram for the model.

For the meaning of the model parameters and the details of their associated assumptions, refer to reference [19]. Let (Ω, F, P) be a discrete probability space satisfying the usual conditions. The DTMC SEIRS-SEIR stochastic model is formulated as a stochastic process $X = \{(E(t,\omega), (I(t,\omega), R(t,\omega))/t \in \mathcal{T}, \omega \in \Omega\} \subset \mathbb{N}^3$, named stochastic realization, where $\mathcal{T}$ is the index set often represents time, such as: $\mathcal{T} = \{0, 1, 2, \ldots\}$, $(E(0,\omega), I(0,\omega), R(0,\omega)) = (e_{t0}, i_{t0}, r_{t0})$, with $i_{t0} \geqslant 1$ and $S(t,\omega) = N - E(t,\omega) - I(t,\omega) - R(t,\omega)$, N is the constant representing the network's total number of nodes (motes). This stochastic process X is composed of two three-dimensional sub-processes X_1 and X_2; the first is the sub-process of the discrete random variables E_1, I_1, R_1 and the second is the sub-process of the discrete random variables E_2, I_2, R_2 such as: for $j = 1, 2$, let $X_j = \{(E_j(t,\omega), (I_j(t,\omega), R_j(t,\omega))/t \in \mathcal{T}, \omega \in \Omega\} \subset \mathbb{N}^3$, with for $j = 1, 2$, let $(E_j(0,\omega), I_j(0,\omega), R_j(0,\omega)) = (e_{jt0}, i_{jt0}, r_{jt0})$, $E_1(t,\omega) + E_2(t,\omega) = E(t,\omega)$, $I_1(t,\omega) + I_2(t,\omega) = I(t,\omega)$ and $R_1(t,\omega) + R_2(t,\omega) = R(t,\omega)$. For simplicity, the sample space notation is canceled and we denote by $E_j(t)$ (respectively $I_j(t)$, and $R_j(t)$) for $j = 1, 2$ a discrete random variables indexed by t for the average number of k_j-degree exposed (respectively infectious, recovered) nodes at discrete-time t.

Let at each time step, $E(t) = E_1(t) + E_2(t)$ (respectively $I(t) = I_1(t) + I_2(t)$, and $R(t) = R_1(t) + R_2(t)$) denotes the discrete random variable S for the average number of exposed (respectively infectious, recovered) nodes at discrete-time t. The other discrete random variables $S_1(t)$, $S_2(t)$, and $S(t)$ can be respectively deduced from the following formulas: $S_1(t) = N_1 - E_1(t) - I_1(t) - R_1(t)$, $S_2(t) = N_2 - E_2(t) - I_2(t) - R_2(t)$, and $S(t) = S_1(t) + S_2(t)$. The state of our DTMC model (SEIRS-SEIR) is entirely defined by $(E(t), (I(t), R(t))$, so by $(E_j(t), (I_j(t), R_j(t)$, for $j = 1, 2\ )$, because each random variable depends on the others. It is therefore sufficient to define a joint probability function of $(E(t), (I(t), R(t))$ and a joint probability function of $(E_j(t), (I_j(t), R_j(t)$, for $j = 1, 2)$ such that:

$$p_{(e_t, i_t, r_t)}(t) = P\{E(t) = e_t, I(t) = i_t, R(t) = r_t\},$$

where $e_t, i_t, r_t = 0, 1, 2, \ldots, N$, $0 \leqslant e_t + i_t + r_t \leqslant N$ and $s_t = N - e_t - i_t - r_t$. This joint function signifies the probability of finding the system with e_t (respectively i_t, r_t) exposed (respectively infectious, recovered) nodes at time t. And,

$$\begin{aligned} &p_{(e_{1t}, i_{1t}, r_{1t}),(e_{2t}, i2t, r_{2t})}(t) \\ &\quad = P\{(E_1(t) = e_{1t}, I_1(t) = i_{1t}, R_1(t) = r_{1t}), (E_2(t) = e_{2t}, I_2(t) = i2t, R_2(t) = r_{2t})\}, \end{aligned}$$

where $e_{jt}, i_{jt}, r_{jt} = 0, 1, 2, \ldots, N_j$, $0 \leqslant e_{jt} + i_{jt} + r_{jt} \leqslant N_j$, $s_{jt} = N_j - e_{jt} - i_{jt} - r_{jt}$, for $j = 1, 2$ and $e_{1t} + e_{2t} = e_t$, $i_{1t} + i_{2t} = i_t$, $r_{1t} + r_{2t} = r_t$, $s_{1t} + s_{2t} = s_t$. This joint function signifies the probability of finding the system with e_{jt} (respectively i_{jt}, r_{jt}) exposed (respectively infectious, recovered) nodes of k_j-degree for $j = 1, 2$ at time t. The notation P is used instead of $P_{(E_1, I_1, R_1),(E_2, I_2, R_2)}(t)$ to denote the induced probability measure. Let Δt be a fixed time interval denoting the period of time between two consecutive times t and $t+\Delta t$, where $t \in \{0, \Delta t, 2\Delta t, \dots\}$. We assume that Δt is small enough such that at most two event and only at most one change in each node state occur during this time. The well-established Markov property, which states that each process at future time $t+\Delta t$ depends solely on the process at the present time t and is independent of the sequence of the past processes, is expressed as follows:

$$\begin{aligned}
&P\big\{\big(E_1(t+\Delta t), I_1(t+\Delta t), R_1(t+\Delta t), E_2(t+\Delta t), I_2(t+\Delta t), R_2(t+\Delta t)\big)|\big(E_1(t), I_1(t), R_1(t),\\
&\quad E_2(t), I_2(t), R_2(t)\big), \dots, \big(E_1(0), I_1(0), R_1(0), E_2(0), I_2(0), R_2(0)\big\}\\
&= P\big\{\big(E_1(t+\Delta t), I_1(t+\Delta t), R_1(t+\Delta t), E_2(t+\Delta t), I_2(t+\Delta t), R_2(t+\Delta t)\big)|\big(E_1(t),\\
&\quad I_1(t), R_1(t), E_2(t), I_2(t), R_2(t)\big)\big\}.
\end{aligned}$$

To finalize the formulation of the DTMC SEIRS-SEIR model for both groups, we establish the interdependence between the states of each random variable and compute the transition probabilities for each event, as outlined below: for each time t we relate all random variables by defining (i) the transition probability during Δt from state $\big(E(t), I(t), R(t)\big) = |m\rangle$ to state $\big(E(t+\Delta t), I(t+\Delta t), R(t+\Delta t)\big) = |n\rangle$, $|m\rangle \xrightarrow{T^*} |n\rangle$, with $|m\rangle = (e_t, i_t, r_t)$ and $|n\rangle = (e'_t, i'_t, r'_t)$; and (ii) the transition probability during Δt from state $\big(E_j(t), I_j(t), R_j(t)\big) = |m_j\rangle$ to state $\big(E_j(t+\Delta t), I_j(t+\Delta t), R_j(t+\Delta t)\big) = |n_j\rangle$, $|m_j\rangle \xrightarrow{T^*_{j,y}} |n_j\rangle$, with $|m_j\rangle = (e_{jt}, i_{jt}, r_{jt})$ and $|n\rangle = (e'_{jt}, i'_{jt}, r'_{jt})$, for $j = 1, 2$, such that we will see later that the index y in $T^*_{j,y}$ will be replaced by e^*_j, r^*_j, 0 and the exponent $*$ in T^*, $T^*_{j,y}$, e^*_j, r^*_j will be replaced by $+$, $-$ and without exponent in T^*, $T^*_{j,y}$ only, according to state $|n\rangle$ and $|n_j\rangle$, $j = 1, 2$:

(i) transition $|m\rangle \xrightarrow{T^*} |n\rangle$:

$$p_{|n\rangle,|m\rangle}(t+\Delta t, t) = P\left\{|n\rangle = (e'_t, i'_t, r'_t) \mid |m\rangle = (e_t, i_t, r_t)\right\} = P(T^*);$$

(ii) transition $|m_j\rangle \xrightarrow{T^*_{j,y}} |n_j\rangle$, where $j = 1, 2$:

$$p_{|n_j\rangle,|m_j\rangle}(t+\Delta t, t) = P\left\{|n_j\rangle = (e'_{jt}, i'_{jt}, r'_{jt}) \mid |m_j\rangle = (e_{jt}, i_{jt}, r_{jt})\right\} = P(T^*_{j,y}).$$

$P(T^*)$ and $P(T^*_{j,y})$, will be used hereafter to indicate the simple notations of the transition probabilities. We are now interested in determining the possible states for $|n\rangle$ and $|n_j\rangle$, for $j = 1, 2$ at time $t+\Delta t$ by proceeding as follows: Δt is chosen to be sufficiently small, ensuring that at most one change in the state of the random variable I can occur. This allows us to cope with the formulation of our DTMC model in the following manner: if $I(t) = i_t$, then one of the three following possible states for the infected random variable I can occur at time $t+\Delta t$: $i_t + 1$ or $i_t - 1$ or i_t. Therefore, we define three transitions T^+, T^-, and T for three-dimensional processes $\big(E(t), I(t), R(t)\big)$ such as:

1) $|m\rangle = (e_t, i_t, r_t) \xrightarrow{T^+} |n\rangle = (e'_t, i_t + 1, r'_t)$, with the corresponding probability:

$$P(T^+) = P\left\{|n\rangle = (e'_t, i_t + 1, r'_t) \mid |m\rangle = (e_t, i_t, r_t)\right\};$$

2) $|m\rangle = (e_t, i_t, r_t) \xrightarrow{T^-} |n\rangle = (e'_t, i_t - 1, r'_t)$, with the corresponding probability:

$$P(T^-) = P\left\{|n\rangle = (e'_t, i_t - 1, r'_t) \mid |m\rangle = (e_t, i_t, r_t)\right\};$$

3) $|m\rangle = (e_t, i_t, r_t) \xrightarrow{T} |n\rangle = (e'_t, i_t, r'_t)$, with the corresponding probability:

$$P(T) = P\left\{|n\rangle = (e'_t, i_t, r'_t) \mid |m\rangle = (e_t, i_t, r_t)\right\};$$

4) a variety of multiple transitions with probability equal zero.

Each transition realization above is an intersection between two specific transitions (one is realized in the first set, and the other is carried out in the second). Thus, thirteen possible cases for the model are distinguished (see Appendix). Given the coexistence of two distinct states that both include three random variables $\left(E_1(t), I_1(t), R_1(t)\right)$ and $\left(E_2(t), I_2(t), R_2(t)\right)$, such that at most one of them can undergo a variation during the time step Δt, and at most one change in the state of each random variable can happen during this time interval, hence, the transition probabilities governing our DTMC model can be concisely expressed through the system of equations (3.2) below:

$$
\begin{aligned}
&p_{(|n_1\rangle,|n_2\rangle),(|m_1\rangle,|m_2\rangle)}(t+\Delta t, t)\\
&= \begin{cases}
P_1(\Delta t) = P\left(T^{+}_{1,e_1^-} \cap T_{2,0}\right), & (e'_{1t}, i'_{1t}, r'_{1t}, e'_{2t}, i'_{2t}, r'_{2t}) = (e_{1t}-1, i_{1t}+1, r_{1t}, e_{2t}, i_{2t}, r_{2t}),\\
P_2(\Delta t) = P\left(T_{1,0} \cap T^{+}_{2,0}\right), & (e'_{1t}, i'_{1t}, r'_{1t}, e'_{2t}, i'_{2t}, r'_{2t}) = (e_{1t}, i_{1t}, r_{1t}, e_{2t}, i_{2t}+1, r_{2t}),\\
P_3(\Delta t) = P\left(T_{1,0} \cap T^{+}_{2,e_2^-}\right), & (e'_{1t}, i'_{1t}, r'_{1t}, e'_{2t}, i'_{2t}, r'_{2t}) = (e_{1t}, i_{1t}, r_{1t}, e_{2t}-1, i_{2t}+1, r_{2t}),\\
P_4(\Delta t) = P\left(T^{-}_{1,r_1^+} \cap T_{2,0}\right), & (e'_{1t}, i'_{1t}, r'_{1t}, e'_{2t}, i'_{2t}, r'_{2t}) = (e_{1t}, i_{1t}-1, r_{1t}+1, e_{2t}, i_{2t}, r_{2t}),\\
P_5(\Delta t) = P\left(T_{1,0} \cap T^{-}_{2,r_2^+}\right), & (e'_{1t}, i'_{1t}, r'_{1t}, e'_{2t}, i'_{2t}, r'_{2t}) = (e_{1t}, i_{1t}, r_{1t}, e_{2t}, i_{2t}-1, r_{2t}+1),\\
P_6(\Delta t) = P\left(T_{1,0} \cap T^{-}_{2,0}\right), & (e'_{1t}, i'_{1t}, r'_{1t}, e'_{2t}, i'_{2t}, r'_{2t}) = (e_{1t}, i_{1t}, r_{1t}, e_{2t}, i_{2t}-1, r_{2t}),\\
P_7(\Delta t) = P\left(T_{1,0} \cap T_{2,r_2^-}\right), & (e'_{1t}, i'_{1t}, r'_{1t}, e'_{2t}, i'_{2t}, r'_{2t}) = (e_{1t}, i_{1t}, r_{1t}, e_{2t}, i_{2t}, r_{2t}-1),\\
P_8(\Delta t) = P\left(T_{1,e_1^+} \cap T_{2,0}\right), & (e'_{1t}, i'_{1t}, r'_{1t}, e'_{2t}, i'_{2t}, r'_{2t}) = (e_{1t}+1, i_{1t}, r_{1t}, e_{2t}, i_{2t}, r_{2t}),\\
P_9(\Delta t) = P\left(T_{1,r_1^-} \cap T_{2,0}\right), & (e'_{1t}, i'_{1t}, r'_{1t}, e'_{2t}, i'_{2t}, r'_{2t}) = (e_{1t}, i_{1t}, r_{1t}-1, e_{2t}, i_{2t}, r_{2t}),\\
P_{10}(\Delta t) = P\left(T_{1,0} \cap T_{2,e_2^+}\right), & (e'_{1t}, i'_{1t}, r'_{1t}, e'_{2t}, i'_{2t}, r'_{2t}) = (e_{1t}, i_{1t}, r_{1t}, e_{2t}+1, i_{2t}, r_{2t}),\\
P_{11}(\Delta t) = P\left(T_{1,0} \cap T_{2,e_2^-}\right), & (e'_{1t}, i'_{1t}, r'_{1t}, e'_{2t}, i'_{2t}, r'_{2t}) = (e_{1t}, i_{1t}, r_{1t}, e_{2t}-1, i_{2t}, r_{2t}),\\
P_{12}(\Delta t) = P\left(T_{1,0} \cap T_{2,0}\right), & (e'_{1t}, i'_{1t}, r'_{1t}, e'_{2t}, i'_{2t}, r'_{2t}) = (e_{1t}, i_{1t}, r_{1t}, e_{2t}, i_{2t}, r_{2t}),\\
0, & \text{otherwise.}
\end{cases}
\end{aligned}
\tag{3.2}
$$

Assuming that the Markov chain is homogeneous over time, the transition probabilities being independent of time, thus:

$$
p_{(|n_1\rangle,|n_2\rangle),(|m_1\rangle,|m_2\rangle)}(t+\Delta t, t) = p_{(|n_1\rangle,|n_2\rangle),(|m_1\rangle,|m_2\rangle)}(\Delta t).
$$

After having computed transition probabilities of the system (3.2), $P_j(\Delta t)$ $(j = 1, \ldots, 12)$, by following the method in references [14, 15] (see the Appendix), the system of equations (3.2) will be rewritten as shown in the equation (3.4) below. Thus, the difference equation satisfied by the probability $p_{|m_1\rangle,|m_2\rangle}(t+\Delta t, t)$, where $|m_1\rangle = (e_{1t}, i_{1t}, r_{1t})$ and $|m_2\rangle = (e_{2t}, i_{2t}, r_{2t})$ can be expressed as a function of the probabilities at time t as given by equations (3.3) and (3.6) below:

$$
\begin{aligned}
&p_{((e_{1t},i_{1t},r_{1t}),(e_{2t},i_{2t},r_{2t}))}(t+\Delta t)\\
&= \Pi_1(\Delta t).p_{((e_{1t},i_{1t}-1,r_{1t}),(e_{2t},i_{2t},r_{2t}))}(t) + \Pi_2(\Delta t).p_{((e_{1t},i_{1t},r_{1t}),(e_{2t},i_{2t}-1,r_{2t}))}(t)\\
&\quad + \Pi_3(\Delta t).p_{((e_{1t},i_{1t},r_{1t}),(e_{2t}+1,i_{2t}-1,r_{2t}))}(t) + \Pi_4(\Delta t).p_{((e_{1t},i_{1t}+1,r_{1t}-1),(e_{2t},i_{2t},r_{2t}))}(t)\\
&\quad + \Pi_5(\Delta t).p_{((e_{1t},i_{1t},r_{1t}),(e_{2t},i_{2t}+1,r_{2t}-1))}(t) + \Pi_6(\Delta t).p_{((e_{1t},i_{1t},r_{1t}),(e_{2t},i_{2t}+1,r_{2t}))}(t)\\
&\quad + \Pi_7(\Delta t).p_{((e_{1t},i_{1t},r_{1t}),(e_{2t},i_{2t},r_{2t}+1))}(t) + \Pi_8(\Delta t).p_{((e_{1t}-1,i_{1t},r_{1t}),(e_{2t},i_{2t},r_{2t}))}(t)\\
&\quad + \Pi_9(\Delta t).p_{((e_{1t},i_{1t},r_{1t}+1),(e_{2t},i_{2t},r_{2t}))}(t) + \Pi_{10}(\Delta t).p_{((e_{1t},i_{1t},r_{1t}),(e_{2t}-1,i_{2t},r_{2t}))}(t)\\
&\quad + \Pi_{11}(\Delta t).p_{((e_{1t},i_{1t},r_{1t}),(e_{2t}+1,i_{2t},r_{2t}))}(t) + \Pi_{12}(\Delta t).p_{((e_{1t},i_{1t},r_{1t}),(e_{2t},i_{2t},r_{2t}))}(t),
\end{aligned}
\tag{3.3}
$$

$$p_{(|n_1\rangle,|n_2\rangle),(|m_1\rangle,|m_2\rangle)}(\Delta t) = \begin{cases} P_1(\Delta t) = \alpha e_{1t}\Delta t\{1-[\eta_2 N_2 + \alpha e_{2t} + \beta k_2 \Theta(i_{1t}, i_{2t})(N_2 - e_{2t} - i_{2t} - r_{2t}) + \mu(e_{2t}+r_{2t}) + (\mu+\gamma) i_{2t}]\Delta t\}, \\ \quad (e'_{1t}, i'_{1t}, r'_{1t}, e'_{2t}, i'_{2t}, r'_{2t}) = (e_{1t}-1, i_{1t}+1, r_{1t}, e_{2t}, i_{2t}, r_{2t}), \\ P_2(\Delta t) = \{1-[\delta r_{1t} + \gamma i_{1t} + \alpha e_{1t} + \beta k_1 \Theta(i_{1t}, i_{2t}+1)(N_1 - e_{1t} - i_{1t} - r_{1t})]\Delta t\}\eta_2 N_2 \Delta t, \\ \quad (e'_{1t}, i'_{1t}, r'_{1t}, e'_{2t}, i'_{2t}, r'_{2t}) = (e_{1t}, i_{1t}, r_{1t}, e_{2t}, i_{2t}+1, r_{2t}), \\ P_3(\Delta t) = \{1-[\delta r_{1t} + \gamma i_{1t} + \alpha e_{1t} + \beta k_1 \Theta(i_{1t}, i_{2t}+1)(N_1 - e_{1t} - i_{1t} - r_{1t})]\Delta t\}\alpha e_{2t} \Delta t, \\ \quad (e'_{1t}, i'_{1t}, r'_{1t}, e'_{2t}, i'_{2t}, r'_{2t}) = (e_{1t}, i_{1t}, r_{1t}, e_{2t}-1, i_{2t}+1, r_{2t}), \\ P_4(\Delta t) = \alpha i_{1t}\Delta t\{1-[\eta_2 N_2 + \alpha e_{2t} + \beta k_2 \Theta(i_{1t}, i_{2t})(N_2 - e_{2t} - i_{2t} - r_{2t}) + \mu(e_{2t}+r_{2t}) + (\mu+\gamma) i_{2t}]\Delta t\}, \\ \quad (e'_{1t}, i'_{1t}, r'_{1t}, e'_{2t}, i'_{2t}, r'_{2t}) = (e_{1t}, i_{1t}-1, r_{1t}+1, e_{2t}, i_{2t}, r_{2t}), \\ P_5(\Delta t) = \{1-[\delta r_{1t} + \gamma i_{1t} + \alpha e_{1t} + \beta k_1 \Theta(i_{1t}, i_{2t}-1)(N_1 - e_{1t} - i_{1t} - r_{1t})]\Delta t\}\gamma i_{2t} \Delta t, \\ \quad (e'_{1t}, i'_{1t}, r'_{1t}, e'_{2t}, i'_{2t}, r'_{2t}) = (e_{1t}, i_{1t}, r_{1t}, e_{2t}, i_{2t}-1, r_{2t}+1), \\ P_6(\Delta t) = \{1-[\delta r_{1t} + \gamma i_{1t} + \alpha e_{1t} + \beta k_1 \Theta(i_{1t}, i_{2t}-1)(N_1 - e_{1t} - i_{1t} - r_{1t})]\Delta t\}\mu i_{2t} \Delta t, \\ \quad (e'_{1t}, i'_{1t}, r'_{1t}, e'_{2t}, i'_{2t}, r'_{2t}) = (e_{1t}, i_{1t}, r_{1t}, e_{2t}, i_{2t}-1, r_{2t}), \\ P_7(\Delta t) = \{1-[\delta r_{1t} + \gamma i_{1t} + \alpha e_{1t} + \beta k_1 \Theta(i_{1t}, i_{2t})(N_1 - e_{1t} - i_{1t} - r_{1t})]\Delta t\}\mu r_{2t} \Delta t, \\ \quad (e'_{1t}, i'_{1t}, r'_{1t}, e'_{2t}, i'_{2t}, r'_{2t}) = (e_{1t}, i_{1t}, r_{1t}, e_{2t}, i_{2t}, r_{2t}-1), \\ P_8(\Delta t) = \beta k_1 \Theta(i_{1t}, i_{2t})(N_1 - e_{1t} - i_{1t} - r_{1t})\Delta t\{1-[\eta_2 N_2 + \alpha e_{2t} + \beta k_2 \Theta(i_{1t}, i_{2t}) \\ \qquad \times (N_2 - e_{2t} - i_{2t} - r_{2t}) + \mu(e_{2t}+r_{2t}) + (\mu+\gamma) i_{2t}]\Delta t\}, \\ \quad (e'_{1t}, i'_{1t}, r'_{1t}, e'_{2t}, i'_{2t}, r'_{2t}) = (e_{1t}-1, i_{1t}+1, r_{1t}, e_{2t}, i_{2t}, r_{2t}), \\ P_9(\Delta t) = \eta r_{1t}\Delta t\{1-[\eta_2 N_2 + \alpha e_{2t} + \beta k_2 \Theta(i_{1t}, i_{2t})(N_2 - e_{2t} - i_{2t} - r_{2t}) + \mu(e_{2t}+r_{2t}) + (\mu+\gamma) i_{2t}]\Delta t\}, \\ \quad (e'_{1t}, i'_{1t}, r'_{1t}, e'_{2t}, i'_{2t}, r'_{2t}) = (e_{1t}, i_{1t}, r_{1t}-1, e_{2t}, i_{2t}, r_{2t}), \\ P_{10}(\Delta t) = \{1-[\delta r_{1t} + \gamma i_{1t} + \alpha e_{1t} + \beta k_1 \Theta(i_{1t}, i_{2t})(N_1 - e_{1t} - i_{1t} - r_{1t})]\Delta t\}\beta k_2 \Theta(i_{1t}, i_{2t}) \\ \qquad \times (N_2 - e_{2t} - i_{2t} - r_{2t})\Delta t, \quad (e'_{1t}, i'_{1t}, r'_{1t}, e'_{2t}, i'_{2t}, r'_{2t}) = (e_{1t}, i_{1t}, r_{1t}, e_{2t}+1, i_{2t}, r_{2t}), \\ P_{11}(\Delta t) = \{1-[\delta r_{1t} + \gamma i_{1t} + \alpha e_{1t} + \beta k_1 \Theta(i_{1t}, i_{2t})(N_1 - e_{1t} - i_{1t} - r_{1t})]\Delta t\}\mu e_{2t} \Delta t, \\ \quad (e'_{1t}, i'_{1t}, r'_{1t}, e'_{2t}, i'_{2t}, r'_{2t}) = (e_{1t}, i_{1t}, r_{1t}, e_{2t}-1, i_{2t}, r_{2t}), \\ P_{12}(\Delta t) = 1 - \sum_{j=1}^{11} P_j(\Delta t), \quad (e'_{1t}, i'_{1t}, r'_{1t}, e'_{2t}, i'_{2t}, r'_{2t}) = (e_{1t}, i_{1t}, r_{1t}, e_{2t}, i_{2t}, r_{2t}), \\ 0, \quad \text{otherwise.} \end{cases} \tag{3.4}$$

3.2. *SDE model*

In practical scenarios, the parameters within a compartmental model are inherently subject to random variations, which influence the population dynamics. Various forms of noise can capture this environmental randomness, and numerous studies have indicated that white noise serves as an appropriate representation for environmental variability in terrestrial systems (refer to Steele 1985 [43]). Therefore, we introduce Gaussian white noise disturbances into this model to account for situations where the parameters μ and δ undergo random fluctuations. To achieve this, we apply the technique of parameter perturbation, a commonly employed approach in constructing stochastic differential equation (SDE) models (as seen in works like Zhang et al. [49]). Specifically, we replace δ with $\delta + \sigma_1 dB_1$ and μ with $\mu + \sigma_2 dB_2$, where $B_1(t)$ and $B_2(t)$ represent standard one-dimensional independent Brownian motions, and σ_1 and σ_2 denote their respective intensities. The remaining parameters remain consistent with those in system (3.1), which gives the stochastic system (3.5) as follows:

$$\begin{cases} dE_1(t) = (k_1\beta(N_1 - E_1(t) - I_1(t) - R_1(t))\Theta(I_1(t), I_2(t)) - \alpha E_1(t))dt, \\ dI_1(t) = (\alpha E_1(t) - \gamma I_1(t))dt, \\ dR_1(t) = (\gamma I_1(t) - \delta R_1(t))dt - \sigma_1 R_1(t) dB_1(t), \\ dE_2(t) = (k_2\beta(N_2 - E_2(t) - I_2(t) - R_2(t))\Theta(I_1(t), I_2(t)) - \alpha E_2(t) - \mu E_2(t))dt - \sigma_2 E_2(t) dB_2(t), \\ dI_2(t) = (\eta_2 N_2 + \alpha E_2(t) - \gamma I_2(t) - \mu I_2(t))dt - \sigma_2 I_2(t) dB_2(t), \\ dR_2(t) = (\gamma I_2(t) - \mu R_2(t))dt - \sigma_2 R_2(t) dB_2(t), \end{cases} \tag{3.5}$$

$$\begin{cases} \Pi_1(\Delta t) = \alpha(e_{1t}+1)\Delta t\{1-[\eta_2 N_2 + \alpha e_{2t} + \beta k_2 \Theta(i_{1t}-1, i_{2t})(N_2 - e_{2t} - i_{2t} - r_{2t}) + \mu(e_{2t}+r_{2t}) + (\mu+\gamma) i_{2t}]\Delta t\}, \\ \Pi_2(\Delta t) = \{1-[\delta r_{1t} + \gamma i_{1t} + \alpha e_{1t} + \beta k_1 \Theta(i_{1t}, i_{2t}-1)(N_1 - e_{1t} - i_{1t} - r_{1t})]\Delta t\}\eta_2 N_2 \Delta t, \\ \Pi_3(\Delta t) = \{1-[\delta r_{1t} + \gamma i_{1t} + \alpha e_{1t} + \beta k_1 \Theta(i_{1t}, i_{2t}-1)(N_1 - e_{1t} - i_{1t} - r_{1t})]\Delta t\}\alpha(e_{2t}+1)\Delta t, \\ \Pi_4(\Delta t) = \alpha(i_{1t}+1)\Delta t\{1-[\eta_2 N_2 + \alpha e_{2t} + \beta k_2 \Theta(i_{1t}+1, i_{2t})(N_2 - e_{2t} - i_{2t} - r_{2t}) + \mu(e_{2t}+r_{2t}) + (\mu+\gamma) i_{2t}]\Delta t\}, \\ \Pi_5(\Delta t) = \{1-[\delta r_{1t} + \gamma i_{1t} + \alpha e_{1t} + \beta k_1 \Theta(i_{1t}, i_{2t}+1)(N_1 - e_{1t} - i_{1t} - r_{1t})]\Delta t\}\gamma i_{2t} \Delta t, \\ \Pi_6(\Delta t) = \{1-[\delta r_{1t} + \gamma i_{1t} + \alpha e_{1t} + \beta k_1 \Theta(i_{1t}, i_{2t}+1)(N_1 - e_{1t} - i_{1t} - r_{1t})]\Delta t\}\mu(i_{2t}+1)\Delta t, \\ \Pi_7(\Delta t) = \{1-[\delta r_{1t} + \gamma i_{1t} + \alpha e_{1t} + \beta k_1 \Theta(i_{1t}, i_{2t})(N_1 - e_{1t} - i_{1t} - r_{1t})]\Delta t\}\mu(r_{2t}+1)\Delta t, \\ \Pi_8(\Delta t) = \beta k_1 \Theta(i_{1t}, i_{2t})(N_1 - e_{1t} + 1 - i_{1t} - r_{1t})\Delta t\{1-[\eta_2 N_2 + \alpha e_{2t} + \beta k_2 \Theta(i_{1t}, i_{2t})(N_2 - e_{2t} - i_{2t} - r_{2t}) \\ \qquad + \mu(e_{2t}+r_{2t}) + (\mu+\gamma) i_{2t}]\Delta t\}, \\ \Pi_9(\Delta t) = \eta(r_{1t}+1)\Delta t\{1-[\eta_2 N_2 + \alpha e_{2t} + \beta k_2 \Theta(i_{1t}, i_{2t})(N_2 - e_{2t} - i_{2t} - r_{2t}) + \mu(e_{2t}+r_{2t}) + (\mu+\gamma) i_{2t}]\Delta t\}, \\ \Pi_{10}(\Delta t) = \{1-[\delta r_{1t} + \gamma i_{1t} + \alpha e_{1t} + \beta k_1 \Theta(i_{1t}, i_{2t})(N_1 - e_{1t} - i_{1t} - r_{1t})]\Delta t\}\beta k_2 \Theta(i_{1t}, i_{2t})(N_2 - e_{2t} + 1 - i_{2t} - r_{2t})\Delta t, \\ \Pi_{11}(\Delta t) = \{1-[\delta r_{1t} + \gamma i_{1t} + \alpha e_{1t} + \beta k_1 \Theta(i_{1t}, i_{2t})(N_1 - e_{1t} - i_{1t} - r_{1t})]\Delta t\}\mu(e_{2t}+1)\Delta t, \\ \Pi_{12}(\Delta t) = 1 - \sum_{j=1}^{11} P_j(\Delta t). \end{cases} \tag{3.6}$$

The transition probabilities $P_j(\Delta t)$, with $j = 1, \ldots, 11$ are given by the system of equations (3.4). In limit cases, we consider $p_{((e_{1t}, i_{1t}, r_{1t}),(e_{2t}, i_{2t}, r_{2t}))}(t)$ as zero when at least one of e_{1t}, i_{1t}, r_{1t}, e_{2t}, i_{2t}, and r_{2t} is negative. We opt to introduce perturbations to the parameters μ and δ because of their pivotal role in shaping the model's dynamics. Their close association with the node-degree k_1 and the node-degree k_2, respectively, and the fact that μ stands out as the most prevalent parameter in equations of the model (3.1), renders them particularly susceptible to external influences, distinguishing them from other parameters. It is imperative that these values of the SDE's solution remain non-negative since they represent physical quantities. Therefore, in order to analyze the dynamic behavior of system (3.5), our initial concern is to determine whether the solution globally and continuously exists while remaining positive throughout its evolution.

The following theorem demonstrates that a solution to SDE (3.5) exists, is global, and remains non-negative.

Theorem 3.1. *For any given initial value* $(E_1(0), I_1(0), R_1(0), E_2(0), I_2(0), R_2(0)) \in \mathbb{R}^6_+$, *there exists a unique positive solution* $(E_1(t), I_1(t), R_1(t), E_2(t), I_2(t), R_2(t))$ *to SDE* (3.5) *on* $t \geqslant 0$. *This solution remains in* $\mathbb{R}^6_+$ *with probability 1.*

Proof. Since the coefficients of model (3.5) satisfy the local Lipschitz condition, then there exist a unique local solution $(E_1(t), I_1(t), R_1(t), E_2(t), I_2(t), R_2(t))$ on $t \in [0, \tau_e)$, where τ_e is the explosion time. Let us prove that this solution is global, i.e., $\tau_e = +\infty$ almost surely (a.s). Let $n_0 > 0$ be sufficiently large for $E_1(0)$,$I_1(0)$, $R_1(0)$, $E_2(0)$, $I_2(0)$ and $R_2(0)$ lying within the interval $[\frac{1}{n_0}, n_0]$. For each integer $n > n_0$, we define the stopping times τ_n as $\tau_n = \inf t \in [0, \tau_e) : \min(E_1(t), I_1(t), R_1(t), E_2(t), I_2(t), R_2(t)) \leqslant \frac{1}{n}$ or $\max E_1(t), I_1(t), R_1(t), E_2(t), I_2(t), R_2(t)) \geqslant n\}$.

Throughout the rest of this paper we set $\inf \emptyset = \infty$, where $\emptyset$ denotes the empty set. One can see that τ_n is increasing as $n \longrightarrow \infty$. Let $\tau_\infty = \lim_{n\to\infty} \tau_n$, thus $\tau_\infty \leqslant \tau_e$ a.s. If we prove that $\tau_\infty = \infty$ a.s, then $\tau_e = \infty$ a.s, thus $(E_1(t), I_1(t), R_1(t), E_2(t), I_2(t), R_2(t)) \in \mathbb{R}^6_+$ a.s. If this statement is false, then there exist a pair of constants $T > 0$ and $\varepsilon \in (0, 1)$ such that $\mathbb{P} \in \{\tau_\infty \leqslant T\} > \varepsilon$. consequently, there exists an integer $n_1 \geqslant n_0$ such that

$$\mathbb{P} \in \{\tau_n \leqslant T\} \geqslant \varepsilon, \quad n \geqslant n_1. \tag{3.7}$$

Let define a C^2-function $V : \mathbb{R}^6_+ \longrightarrow \mathbb{R}_+$ by

$$\begin{aligned} V(E_1, I_1, R_1, E_2, I_2, R_2) = {} & (E_1 - \log E_1) + (I_1 - \log I_1) + (R_1 - \log R_1) \\ & + (E_2 - \log E_2) + (I_2 - \log I_2) + (R_2 - \log R_2). \end{aligned}$$

It is easy to verify that V is a non-negative function. Let $(E_1(t), I_1(t), R_1(t), E_2(t), I_2(t), R_2(t)) = (E_1 - \log E_1) \in \mathbb{R}^6_+$, by application of Ito formula, we have:

$$\begin{aligned}
dV =& \big((1-\frac{1}{E_1})(k_1\beta(N_1-E_1-I_1-R_1)\Theta(I_1,I_2)-\alpha E_1\big)dt + \big((1-\frac{1}{I_1})(\alpha E_1-\gamma I_1\big)dt \\
&+ \big((1-\frac{1}{R_1})(\gamma I_1-\delta R_1)+\frac{1}{2}\sigma_1^2\big)dt + \big((1-\frac{1}{E_2})(k_2\beta\,(N_2-E_2-I_2-R_2)\,\Theta(I_1,I_2) \\
&-\alpha E_2-\mu E_2+\frac{1}{2}\sigma_2^2\big)dt + \big((1-\frac{1}{I_2})(\eta_2 N_2+\alpha E_2-\gamma I_2-\mu I_2)+\frac{1}{2}\sigma_2^2\big)dt + \big((1-\frac{1}{R_2})(\gamma I_2-\mu R_2) \\
&+\frac{1}{2}\sigma_2^2\big)dt + \big((1-\frac{1}{E_2})(-\sigma_2 E_2)+(1-\frac{1}{I_2})(-\sigma_2 I_2) \\
&+(1-\frac{1}{R_2})(-\sigma_2 R_2)\big)dB_2 + (1-\frac{1}{R_1})(-\sigma_1 R_1)\big)dB_1 \\
=& LVdt + (3\sigma_2-\sigma_2(E_2+I_2+R_2))dB_2+\sigma_1(1-R_1))dB_1,
\end{aligned} \tag{3.8}$$

where

$$\begin{aligned}
LV =& k_1\beta(N_1-E_1-I_1-R_1)\Theta(I_1,I_2) - \frac{k_1\beta(N_1-E_1-I_1-R_1)\Theta(I_1,I_2)}{E_1} - \alpha\frac{E_1}{I_1} - \delta R_1 - \gamma\frac{I_1}{R_1} \\
&+ k_2\beta(N_2-E_2-I_2-R_2)\Theta(I_1,I_2) - \mu E_2 - \frac{k_2\beta(N_2-E_2-I_2-R_2)\Theta(I_1,I_2)}{E_2} \\
&+ \eta_2 N_2 - \mu I_2 - \eta\frac{N_2}{I_2} - \alpha\frac{E_2}{I_2} - \mu R_2 - \gamma\frac{I_2}{R_2} + 3\mu + 2\alpha + 2\gamma + \delta + \frac{1}{2}(\sigma_1^2+3\sigma_2^2) \\
\leqslant& k_1\beta N_1\Theta(I_1,I_2) + k_2\beta N_2\Theta(I_1,I_2) + \eta N_2 + 3\mu + 2\alpha + 2\gamma + \delta + \frac{1}{2}(\sigma_1^2+3\sigma_2^2) \\
\leqslant& k_1\beta N_1 + k_2\beta N_2 + \eta N_2 + 3\mu + 2\alpha + 2\gamma + \delta + \frac{1}{2}(\sigma_1^2+3\sigma_2^2) = K.
\end{aligned}$$

By substituting the last inequality into (3.8), we get:

$$dV(E_1,I_1,R_1,E_2,I_2,R_2) + (3\sigma_2-\sigma_2(E_2+I_2+R_2))dB_2 + \sigma(1-R_1)dB_1, \tag{3.9}$$

which gives

$$\begin{aligned}
\int_0^{\tau_n\wedge T} dV(E_1,I_1,R_1,E_2,I_2,R_2) \leqslant& \int_0^{\tau_n\wedge T} Kdt + \int_0^{\tau_n\wedge T} \sigma_2(3-E_2(r)-I_2(r)-R_2(r))dB_2(r) \\
&+ \int_0^{\tau_n\wedge T} \sigma_1(1-R_1(r))dB_1(r),
\end{aligned}$$

where $\tau_n\wedge T=\min\{\tau_n,T\}$. By taking the expectation of the (3.9) we obtain

$$\begin{aligned}
&E[V(E_1(\tau_n\wedge T),I_1(\tau_n\wedge T),R_1(\tau_n\wedge T),E_2(\tau_n\wedge T),I_2(\tau_n\wedge T),R_2(\tau_n\wedge T))] \\
&\quad\leqslant V(E_1(0),I_1(0),R_1(0),E_2(0),I_2(0),R_2(0)) + KT.
\end{aligned} \tag{3.10}$$

Let $\Omega_n=\{\tau_n\leqslant T\}$ for $n\geqslant n_1$, we have from (3.7), $\mathbb{P}(\Omega_n)\geqslant\varepsilon$. Note that for $w\in\Omega_n$, there exists at least one of $E_1(\tau_n,\omega),I_1(\tau_n,\omega),R_1(\tau_n,\omega),E_2(\tau_n,\omega),I_2(\tau_n,\omega)$, and $R_2(\tau_n,\omega)$ equaling n or $\frac{1}{n}$, so, $V(E_1(\tau_n,\omega),I_1(\tau_n,\omega),R_1(\tau_n,\omega),E_2(\tau_n,\omega),I_2(\tau_n,\omega),R_2(\tau_n,\omega))\geqslant(n-1-\log n)\wedge(\frac{1}{n}-1-\log(\frac{1}{n}))$. Therefore, from (3.10), $V(E_1(0),I_1(0),R_1(0),E_2(0),I_2(0),R_2(0))+KT\geqslant E[\chi_{\Omega_n}(\omega)V(E_1(\tau_n),I_1(\tau_n),R_1(\tau_n),$ $E_2(\tau_n),I_2(\tau_n),R_2(\tau_n))]\geqslant\varepsilon((n-1-\log n)\wedge(\frac{1}{n}-1-\log(\frac{1}{n})))$, where χ_{Ω_n} is the indicator function of Ω_n. By letting $n\to\infty$, $\infty>V(E_1(0),I_1(0),R_1(0),E_2(0),I_2(0),R_2(0))+KT=\infty$ a.s, which is a contradiction. So we must have $\tau_\infty=\infty$. Thus, the solution of SDE (3.5) will not explode at a finite time with probability one. This complete the proof of Theorem 3.1. □

Remark 3.2. The previous theorem guarantees the well posedness of the SDE (3.5). One can investigates some other classical questions such as the extinction, the permanence, the persistence in the mean, and the existence of a unique stationary distribution for the infected nodes variable $I(t)$. We note that these concernes are often discussed in the literature and use the SDE background theory (see for instance [11, 13, 27, 35–37]). The investigation of these questions for SDE (3.5) represents a real challenge in our futur papers.

4. Numerical simulation and discussions

To bolster our theoretical findings, we present numerical simulations encompassing both stochastic models (DTMC and SDE) alongside the deterministic counterpart. For the deterministic model, we employ the fourth-order Runge-Kutta method to effectively solve the Ordinary Differential Equation (ODE) as expressed in equation (3.1). Meanwhile, the DTMC model is subjected to simulation using the Monte Carlo method, harnessing its power to provide probabilistic insights. To address the intricacies of the system outlined in equation (3.5) within the stochastic framework, we leverage the Euler-Maruyama method. Furthermore, a comprehensive discussion of these numerical outcomes is presented, accompanied by a comprehensive comparison between all models.

4.1. DTMC model

We proceed the DTMC model with the Algorithm 1. To illustrate its dynamic behavior, we give two examples devoted to the evolution of each stochastic fraction $e_1(t)$, $i_1(t)$, $r_1(t)$, $e_2(t)$, $i_2(t)$, $r_2(t)$, $e(t)$, $i(t)$, and $r(t)$, and we compare them with the deterministic ones. In Example 4.1, we take the same arbitrarily selected network parameters in Example 3 introduced in Ref. [19]. In Example 4.2, we numerically determine the network parameters by modeling the Barabási-Albert scale-free network, and we demonstrate the effect of the network size ($N = 15000$) on the dynamics of the stochastic model. Additionally, we show the effect of model parameters on the total stochastic fraction of infections.

Example 4.1. We consider the case given by the network and model parameters $N_1 = 200$, $N_2 = 300$, $k_1 = 150$, $k_2 = 10$, $\alpha = 0.1$, $\delta = 0.08$, $\mu = 0.05$, $\beta = 0.0005$ and $\gamma = 0.03$, $\eta_2 = 0.0006$. Fig. 2, Fig. 3, and Fig. 4 represent respectively the time plots of exposed fractions, infected fractions, and recovered fractions in both cases (deterministic and stochastic) with a time step $\Delta t = 0.001$, and initial conditions:

$$\begin{aligned}&\left(e_1(0), e_2(0), e(0), i_1(0), i_2(0), i(0), r_1(0), r_2(0), r(0)\right)\\&\quad = (0.1, 0.033, 0.0598, 0.075, 0.1, 0.09, 0.025, 0.0266, 0.02596)\end{aligned}$$

Figures 2, 3, and 4 show the dynamic behavior of DTMC model. Notably, it prominently converges towards a stable viral equilibrium, which aligns with the predictions of the deterministic model. The congruence between these two models becomes strikingly apparent as their solutions closely coincide, especially when the mean of the random realizations significantly increases.

Example 4.2. Consider the case given by the network and model parameters $N_1 = 693$, $N_2 = 14307$, $k_1 = 21.79$, $k_2 = 3.13$, $\alpha = 0.005$, $\delta = 0.002$, $\mu = 0.003$, $\beta = 0.004$, and $\gamma = 0.006$, $\eta_2 = 0.0002$. Fig. 5 represent respectively the time plots of exposed total fractions, infected total fractions, and recovered total fractions in both cases (deterministic and stochastic) with a time step $\Delta t = 0.001$, and initial conditions:

$$\begin{aligned}&\left(e_1(0), e_2(0), e(0), i_1(0), i_2(0), i(0), r_1(0), r_2(0), r(0)\right)\\&\quad = (0.216, 0.454, 0.443, 0.548, 0.258, 0.272, 0.108, 0.1048, 0.105).\end{aligned}$$

Algorithm 1 Algorithm of the DTMC SEIRS-SEIR model

Require: The transition probabilities $P_j(\Delta t)$, with $j = 1, \dots, 6$

Initialize the six random variables E_1, I_1, R_1, E_2, I_2, R_2, E, I, and R, where $E \leftarrow E_1 + E_2$, $I \leftarrow I_1 + I_2$, $R \leftarrow R_1 + R_2$

for $t \leftarrow 1$ to endtime **do**

Generate an uniform random number q in the interval $]0, 1[$

if $q \leqslant P_1(\Delta t)$ **then**

$E_1(t+\Delta t) \leftarrow e_{1t} - 1$, $E_2(t+\Delta t) \leftarrow e_{2t}$, $E(t+\Delta t) \leftarrow e_{1t} + e_{2t} - 1$, $I_1(t+\Delta t) \leftarrow i_{1t} + 1$, $I_2(t+\Delta t) \leftarrow i_{2t}$, $I(t+\Delta t) \leftarrow i_{1t} + i_{2t} + 1$, $R_1(t+\Delta t) \leftarrow r_{1t}$, $R_2(t+\Delta t) \leftarrow r_{2t}$, and $R(t+\Delta t) \leftarrow r_{1t} + r_{2t}$

else if $q \leqslant P_1(\Delta t) + P_2(\Delta t)$ **then**

$E_1(t+\Delta t) \leftarrow e_{1t}$, $E_2(t+\Delta t) \leftarrow e_{2t}$, $E(t+\Delta t) \leftarrow e_{1t} + e_{2t}$, $I_1(t+\Delta t) \leftarrow i_{1t}$, $I_2(t+\Delta t) \leftarrow i_{2t} + 1$, $I(t+\Delta t) \leftarrow i_{1t} + i_{2t} + 1$, $R_1(t+\Delta t) \leftarrow r_{1t}$, $R_2(t+\Delta t) \leftarrow r_{2t}$, and $R(t+\Delta t) \leftarrow r_{1t} + r_{2t}$

else if $q \leqslant P_1(\Delta t) + P_2(\Delta t) + P_3(\Delta t)$ **then**

$E_1(t+\Delta t) \leftarrow e_{1t}$, $E_2(t+\Delta t) \leftarrow e_{2t} - 1$, $E(t+\Delta t) \leftarrow e_{1t} + e_{2t} - 1$, $I_1(t+\Delta t) \leftarrow i_{1t}$, $I_2(t+\Delta t) \leftarrow i_{2t} + 1$, $I(t+\Delta t) \leftarrow i_{1t} + i_{2t} + 1$, $R_1(t+\Delta t) \leftarrow r_{1t}$, $R_2(t+\Delta t) \leftarrow r_{2t}$, and $R(t+\Delta t) \leftarrow r_{1t} + r_{2t}$

else if $q \leqslant \sum_{j=1}^{4} P_j(\Delta t)$ **then**

$E_1(t+\Delta t) \leftarrow e_{1t}$, $E_2(t+\Delta t) \leftarrow e_{2t}$, $E(t+\Delta t) \leftarrow e_{1t} + e_{2t}$, $I_1(t+\Delta t) \leftarrow i_{1t} - 1$, $I_2(t+\Delta t) \leftarrow i_{2t}$, $I(t+\Delta t) \leftarrow i_{1t} + i_{2t} - 1$, $R_1(t+\Delta t) \leftarrow r_{1t} + 1$, $R_2(t+\Delta t) \leftarrow r_{2t}$, and $R(t+\Delta t) \leftarrow r_{1t} + r_{2t} + 1$

else if $q \leqslant \sum_{j=1}^{5} P_j(\Delta t)$ **then**

$E_1(t+\Delta t) \leftarrow e_{1t}$, $E_2(t+\Delta t) \leftarrow e_{2t}$, $E(t+\Delta t) \leftarrow e_{1t} + e_{2t}$, $I_1(t+\Delta t) \leftarrow i_{1t}$, $I_2(t+\Delta t) \leftarrow i_{2t} - 1$, $I(t+\Delta t) \leftarrow i_{1t} + i_{2t} - 1$, $R_1(t+\Delta t) \leftarrow r_{1t}$, $R_2(t+\Delta t) \leftarrow r_{2t} + 1$, and $R(t+\Delta t) \leftarrow r_{1t} + r_{2t} + 1$

else if $q \leqslant \sum_{j=1}^{6} P_j(\Delta t)$ **then**

$E_1(t+\Delta t) \leftarrow e_{1t}$, $E_2(t+\Delta t) \leftarrow e_{2t}$, $E(t+\Delta t) \leftarrow e_{1t} + e_{2t}$, $I_1(t+\Delta t) \leftarrow i_{1t}$, $I_2(t+\Delta t) \leftarrow i_{2t} - 1$, $I(t+\Delta t) \leftarrow i_{1t} + i_{2t} - 1$, $R_1(t+\Delta t) \leftarrow r_{1t}$, $R_2(t+\Delta t) \leftarrow r_{2t}$, and $R(t+\Delta t) \leftarrow r_{1t} + r_{2t}$

else if $q \leqslant \sum_{j=1}^{7} P_j(\Delta t)$ **then**

$E_1(t+\Delta t) \leftarrow e_{1t}$, $E_2(t+\Delta t) \leftarrow e_{2t}$, $E(t+\Delta t) \leftarrow e_{1t} + e_{2t}$, $I_1(t+\Delta t) \leftarrow i_{1t}$, $I_2(t+\Delta t) \leftarrow i_{2t}$, $I(t+\Delta t) \leftarrow i_{1t} + i_{2t}$, $R_1(t+\Delta t) \leftarrow r_{1t}$, $R_2(t+\Delta t) \leftarrow r_{2t} - 1$, and $R(t+\Delta t) \leftarrow r_{1t} + r_{2t} - 1$

else if $q \leqslant \sum_{j=1}^{8} P_j(\Delta t)$ **then**

$E_1(t+\Delta t) \leftarrow e_{1t} + 1$, $E_2(t+\Delta t) \leftarrow e_{2t}$, $E(t+\Delta t) \leftarrow e_{1t} + e_{2t} + 1$, $I_1(t+\Delta t) \leftarrow i_{1t}$, $I_2(t+\Delta t) \leftarrow i_{2t}$, $I(t+\Delta t) \leftarrow i_{1t} + i_{2t}$, $R_1(t+\Delta t) \leftarrow r_{1t}$, $R_2(t+\Delta t) \leftarrow r_{2t}$, and $R(t+\Delta t) \leftarrow r_{1t} + r_{2t}$

else if $q \leqslant \sum_{j=1}^{9} P_j(\Delta t)$ **then**

$E_1(t+\Delta t) \leftarrow e_{1t}$, $E_2(t+\Delta t) \leftarrow e_{2t}$, $E(t+\Delta t) \leftarrow e_{1t} + e_{2t}$, $I_1(t+\Delta t) \leftarrow i_{1t}$, $I_2(t+\Delta t) \leftarrow i_{2t}$, $I(t+\Delta t) \leftarrow i_{1t} + i_{2t}$, $R_1(t+\Delta t) \leftarrow r_{1t} - 1$, $R_2(t+\Delta t) \leftarrow r_{2t}$, and $R(t+\Delta t) \leftarrow r_{1t} + r_{2t} - 1$

else if $q \leqslant \sum_{j=1}^{10} P_j(\Delta t)$ **then**

$E_1(t+\Delta t) \leftarrow e_{1t}$, $E_2(t+\Delta t) \leftarrow e_{2t} + 1$, $E(t+\Delta t) \leftarrow e_{1t} + e_{2t} + 1$, $I_1(t+\Delta t) \leftarrow i_{1t}$, $I_2(t+\Delta t) \leftarrow i_{2t}$, $I(t+\Delta t) \leftarrow i_{1t} + i_{2t}$, $R_1(t+\Delta t) \leftarrow r_{1t}$, $R_2(t+\Delta t) \leftarrow r_{2t}$, and $R(t+\Delta t) \leftarrow r_{1t} + r_{2t}$

else if $q \leqslant \sum_{j=1}^{11} P_j(\Delta t)$ **then**

$E_1(t+\Delta t) \leftarrow e_{1t}$, $E_2(t+\Delta t) \leftarrow e_{2t} - 1$, $E(t+\Delta t) \leftarrow e_{1t} + e_{2t} - 1$, $I_1(t+\Delta t) \leftarrow i_{1t}$, $I_2(t+\Delta t) \leftarrow i_{2t}$, $I(t+\Delta t) \leftarrow i_{1t} + i_{2t}$, $R_1(t+\Delta t) \leftarrow r_{1t}$, $R_2(t+\Delta t) \leftarrow r_{2t}$, and $R(t+\Delta t) \leftarrow r_{1t} + r_{2t}$

else

$E_1(t+\Delta t) \leftarrow e_{1t}$, $E_2(t+\Delta t) \leftarrow e_{2t}$, $E(t+\Delta t) \leftarrow e_{1t} + e_{2t}$, $I_1(t+\Delta t) \leftarrow i_{1t}$, $I_2(t+\Delta t) \leftarrow i_{2t}$, $I(t+\Delta t) \leftarrow i_{1t} + i_{2t}$, $R_1(t+\Delta t) \leftarrow r_{1t}$, $R_2(t+\Delta t) \leftarrow r_{2t}$, and $R(t+\Delta t) \leftarrow r_{1t} + r_{2t}$

end if

end for

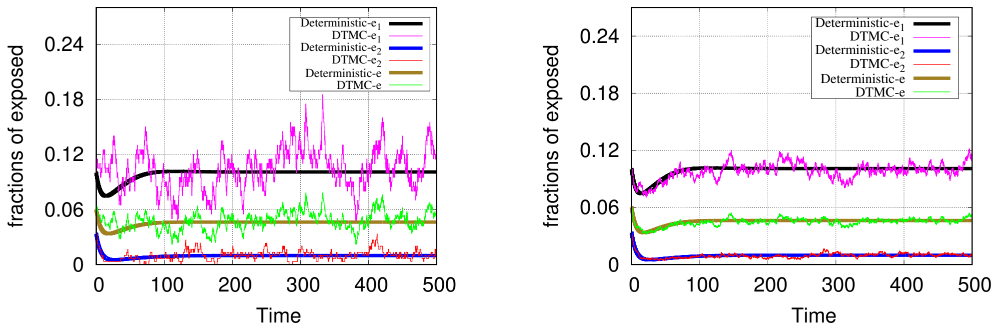

(a) (b)

Figure 2: Evolution of the three total fractions of exposed for the DTMC model with time together with the corresponding solutions of the deterministic model (smooth curves); (a) correspond to a single stochastic realization, and (b) correspond to the mean of 10 stochastic realizations.

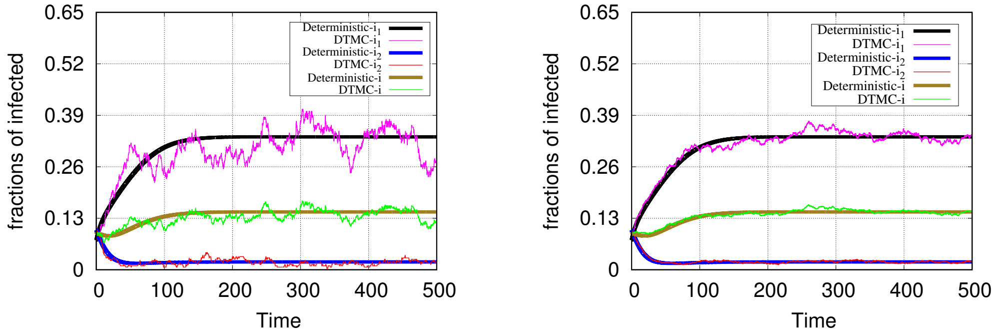

(a) (b)

Figure 3: The three numerical means of the total fractions of infected as function of time for the DTMC model versus the solutions of the deterministic ones; (a) and (b) correspond respectively to a single stochastic realization and to the mean of 10 stochastic realizations.

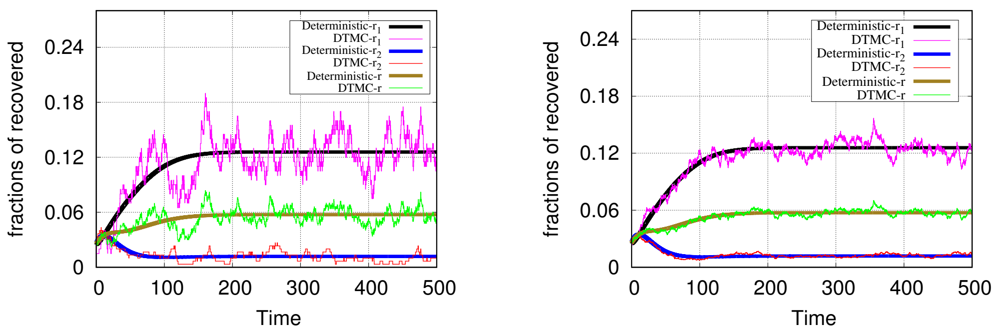

(a) (b)

Figure 4: The temporal evolution of the three numerical means of recovered fractions in the DTMC model are compared to their deterministic solutions (smooth plots): (a) correspond to a single stochastic realization, while (b) (blue curves) show the mean of 10 stochastic realizations.

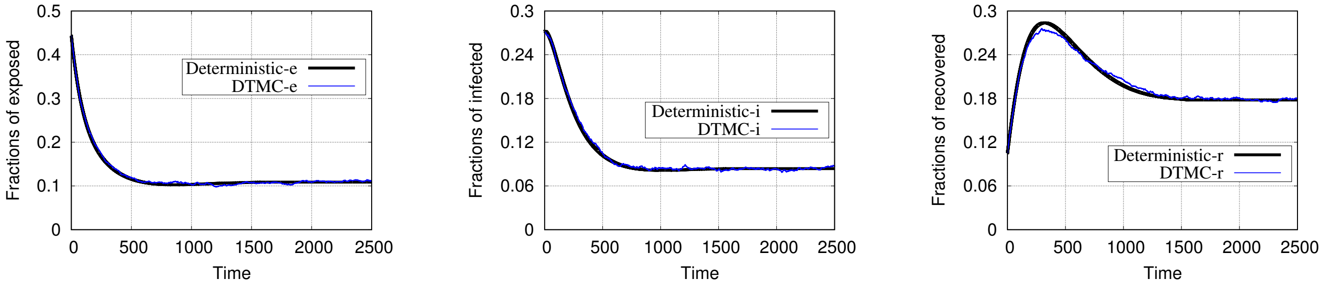

(a) (b) (c)

Figure 5: The temporal evolution of the total fractions of exposed, infected, and recovered in the DTMC model is illustrated alongside the corresponding solutions of the deterministic model for a single stochastic realization.

Figure 5 demonstrates that, despite a substantial population size (comprising a significant number of nodes), the dynamic behavior of the DTMC model consistently converges to a stable viral equilibrium, aligning with the deterministic model's predictions. We also observed a notable reduction in fluctuations within the DTMC model when we employed a simulation of a Barabási-Albert scale-free network to derive the network parameters compared to Example 4.1, where the authors used arbitrary parameters of a reduced scale-free network. Furthermore, the virus extinction is unattainable regardless of the network's size. This underscores the impracticality of completely eradicating all viruses from the WSN. However, an alternative approach entails implementing effective measures to sustain a more balanced energy consumption profile and fortify the WSN's resilience against potential failures. Figure 6 confirms that as follows.

(i) as depicted in Figure 6 (a), elevating the outgoing rate of motes μ leads to a decline in the count of infected sensor nodes. Consequently, it is highly recommended to enhance the departure probability of the lowly linked infected sensor nodes from the sensor field by integrating some strategies such as: implementing self-healing mechanisms that automatically isolate or remove the lowly linked infected motes. This will enhance the probability of those motes departing from the sensor field. Use behavioral analysis to identify potentially the lowly linked infected motes and remove them from the network before the infection spreads. Enable sensing the lowly linked sensor nodes to collaborate for collective defense by sharing information about infections and taking collective action to increase the probability of departure.

(ii) Decreasing the incoming rate of infected motes η_2 is beneficial in reducing infection (see Figure 6 (b)). Therefore, we recommend taking the following measures: ensuring that incoming infected sensor nodes receive timely updates and patches to address vulnerabilities, reducing the likelihood of successful infections. Using intrusion prevention techniques to prevent or mitigate attempts by infected motes to infiltrate the sensor field. Implement robust encryption, authentication, and intrusion detection systems to deter and identify potential threats from infected motes to enhance the security of the sensor network.

(iii) Enhancing the cure rate γ can help stop malware spread (see Figure 6 (c)). For example, regular updates and patches for infected sensor nodes can address vulnerabilities, reducing the likelihood of infection and facilitating smoother recovery. Algorithms can also be introduced to enable these motes to independently detect and recover from infections, boosting overall recovery probability.

(iv) Reducing the exposure rate β or infection rate α can help reduce the prevalence of malware (refer to Figs. 6 (d), (e)). To achieve this, it is crucial to ensure timely updates and patches for susceptible and exposed sensor nodes to address vulnerabilities and minimize the risk of infection. Additionally, educating users and administrators about security best practices can help minimize unintentional actions that could lead to exposure or infection.

(v) The predominance of the malware is decreased by reducing the susceptibility rate δ (see Figure 6 (f)). As previously mentioned, it is essential to strengthen encryption and authentication protocols to protect against unauthorized access. Additionally, regular updates and patching should be ensured for recovered hubs to limit their re-infection.

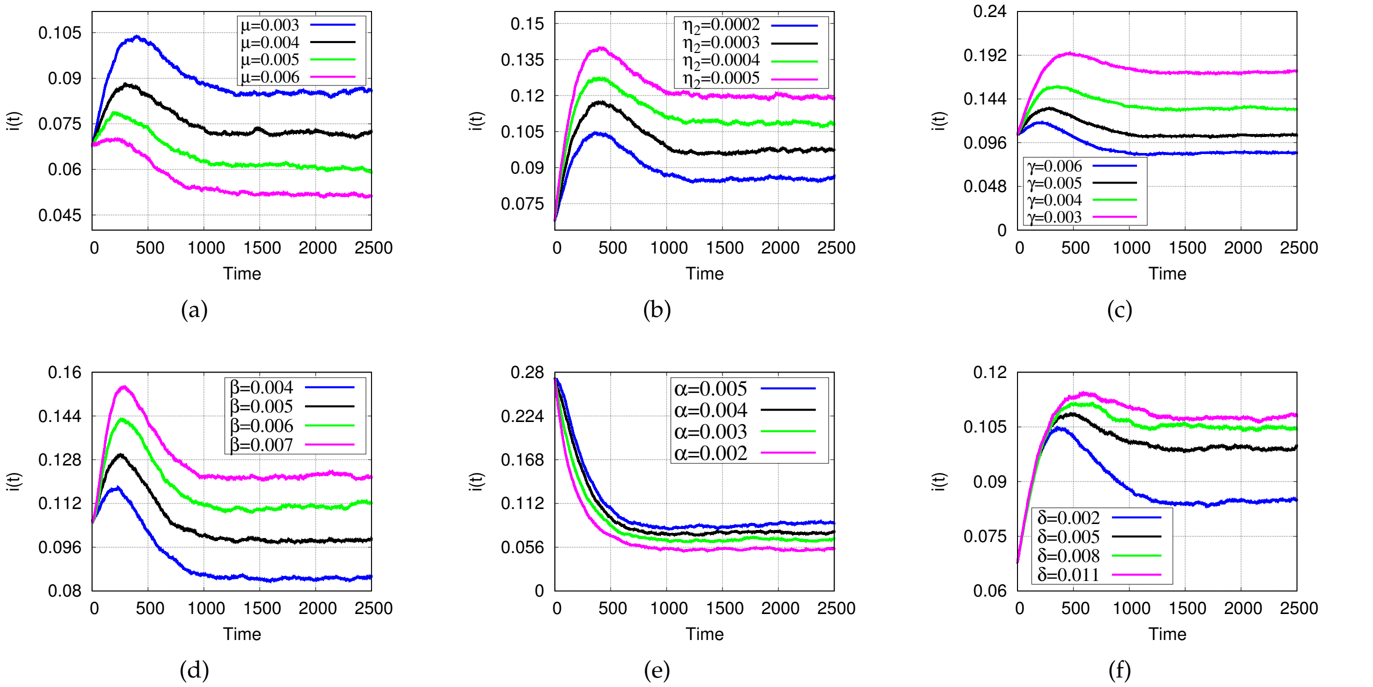

Figure 6: Impact of the different values of the model parameters (μ, η_2, γ, β, α, *and* δ) on the average total density of infected sensors per unit of time, on the average total density of infected per unit time.

4.2. SDE model

To illustrate the dynamic behavior of SDE model (3.5), we propose an example given by the following parameters.

Example 4.3. We set $N_1 = 200$, $N_2 = 300$, $k_1 = 150$, $k_2 = 10$, $\alpha = 0.1$, $\delta = 0.08$, $\mu = 0.05$, $\beta = 0.0005$, $\gamma = 0.03$, $\eta_2 = 0.0006$, $\sigma_1 = 0.05$, $\sigma_2 = 0.08$, and $\Delta t = 0.001$. The parameters of Example 4.3 are chosen arbitrary, numerical simulation in Fig. 7 shows the paths of e, i, and r in both cases (deterministic, DTMC, and SDE) by using the parameters of Example 4.3, and the initial conditions:

$$\begin{aligned}&\left(e_1(0), e_2(0), e(0), i_1(0), i_2(0), i(0), r_1(0), r_2(0), r(0)\right)\\&\quad=(0.1, 0.033, 0.0598, 0.075, 0.1, 0.09, 0.025, 0.0266, 0.02596).\end{aligned}$$

First, simulations support the positivity and the uniqueness of the model's solution (3.5), as shown in Theorem 3.1. Second, some other properties have been identified from simulations but need theoretical proof (which will be the objective of a future paper).

(1) A big concordance between the deterministic curve, the DTMC curve, and the SDE curve. The alignment between the deterministic curve and the SDE curve is more evident in Figures 7 (a) and (b) than the alignment between the deterministic curve and the DTMC curve. This distinction is attributed to the substantial fluctuations in the DTMC model as opposed to the smoother behavior of the SDE model. However, in Figure 7 (c), both models exhibit nearly identical fluctuation patterns.

(2) A remarkable stability of the deterministic model (black curves) and the SDE model (blue curves) over long periods.

(3) As for the deterministic model, there are no extinction times for the SDE model and DTMC model. These perspectives need to be confirmed theoretically in a future paper.

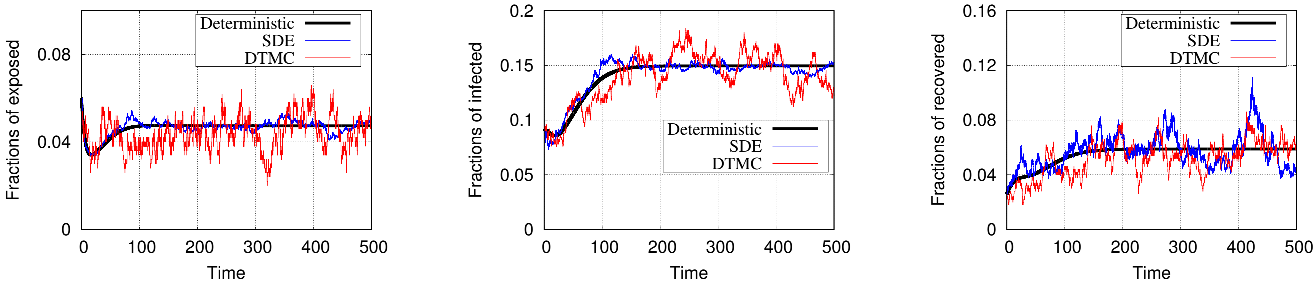

Figure 7: The temporal evolution of the total fractions of exposed, infected, and recovered in both the DTMC and SDE models, along with their corresponding solutions in the deterministic model (smooth curves), are depicted for a single stochastic realization.

5. Conclusion

Our work aims to bring realism to the modeling of malware propagation in reduced scale-free topology-based wireless sensor networks. This is achieved by introducing a stochastic approach, acknowledging the omnipresence of randomness in real-world scenarios. We employed two distinct methodologies, the discrete-time Markov chain (DTMC) and stochastic differential equation (SDE) techniques.

On the one hand, we have shown how various model parameters influence the overall infection dynamics within these networks. Our work went a step further by validating the credibility of our stochastic models, demonstrating their consistency and the extent of their fluctuations in comparison to the deterministic approach. This comparative study provides crucial insights into the impact of stochastic fluctuations on the dynamics of malware propagation in WSNs.

On the other hand, in the real world, problems often exhibit non-deterministic behavior and incorporating stochastic effects into a model can enhance its accuracy when investigating various phenomena. The technique of the perturbation of parameters is considered one of the significant techniques that permit to integration of stochastic fluctuations into a deterministic model. A full section of our work has been dedicated to studying a stochastic version of the model (3.1) created by the parameters perturbation technique. First, the solution’s existence, globality, and uniqueness have been proven, which validates the well-posedness of the stochastic model. Next, throughout a numerical simulation, we have provided a preliminary perspective on the stochastic stability of the solution. This last result is significant, however, simulation alone cannot be relied upon to prove this hypothesis. The theoretical proof remains a significant perspective challenge in an upcoming paper. The results of this latest approach exhibited a high degree of consistency with those derived from the DTMC method, bolstering our confidence and certainty in the findings, especially when they agree with the deterministic approach.

Our findings also underscore the advantages of implementing specific countermeasures within the WSNs. After implementing these countermeasures, we have observed significant improvements in the network’s overall resilience against faults and a more balanced power consumption, attributed to the decreased number of infected sensing devices. This research establishes a meticulous and systematic probabilistic framework, offering a profound understanding of the intricate randomness inherent in the behavioral patterns of malware within wireless sensor networks. These insights contribute to advancing network security strategies and management practices in the face of evolving threats.

In future research, we aim to improve our models by incorporating greater realism. Specifically, we plan to explore models like SEIR-SEIR and SEIR-SEIR-SI, which include multiple sub-chains with high dimensions constructed on a scale-free network or its variations and incorporate three categories of nodes. Our methodology will extend to utilizing continuous-time Markov chains (CTMC), introducing intricate dependencies that encompass perturbing model parameters, and incorporating non-linear dependence probabilities, thereby capturing more nuanced aspects of the system dynamics. In addition, our framework can be extended to describe different dissemination processes, such as the spread of diseases, opinions, and rumors on social media. This expansion will enhance our understanding of complex dynamic systems.

Appendix

(A) Relationship between all states of each random variable

Case (1): The transition T^+ can take place if the two following transitions T^+_{1,e_1^-} and $T_{2,0}$ or two following transitions $T_{1,0}$ and $T^+_{2,0}$ or two following transitions $T_{1,0}$ and T^+_{2,e_2^-} are carried simultaneously:

$$|m_1\rangle = (e_{1t}, i_{1t}, r_{1t}) \overset{T^+_{1,e_1^-}}{\rightarrow} |n_1\rangle = (e_{1t}-1, i_{1t}+1, r_{1t}) \text{ and } |m_2\rangle = (e_{2t}, i_{2t}, r_{2t}) \overset{T_{2,0}}{\rightarrow} |n_2\rangle = (e_{2t}, i_{2t}, r_{2t}),$$

with the corresponding probability:

$$\begin{aligned} &P\left(T^+_{1,e_1^-} \cap T_{2,0}\right) \\ &= P\left\{|n_1\rangle = (e_{1t}-1, i_{1t}+1, r_{1t}) \mid |m_1\rangle = (e_{1t}, i_{1t}, r_{1t}) \cap |n_2\rangle = (e_{2t}, i_{2t}, r_{2t}) \mid |m_2\rangle = (e_{2t}, i_{2t}, r_{2t})\right\} \end{aligned} \tag{.1}$$

or $|m_1\rangle = (e_{1t}, i_{1t}, r_{1t}) \overset{T_{1,0}}{\rightarrow} |n_1\rangle = (e_{1t}, i_{1t}, r_{1t})$ and $|m_2\rangle = (e_{2t}, i_{2t}, r_{2t}) \overset{T^+_{2,0}}{\rightarrow} |n_2\rangle = (e_{2t}, i_{2t}+1, r_{2t})$, with the corresponding probability:

$$\begin{aligned} &P\left(T_{1,0} \cap T^+_{2,0}\right) \\ &= P\left\{|n_1\rangle = (e_{1t}, i_{1t}, r_{1t}) \mid |m_1\rangle = (e_{1t}, i_{1t}, r_{1t}) \cap |n_2\rangle = (e_{2t}, i_{2t}+1, r_{2t}) \mid |m_2\rangle = (e_{2t}, i_{2t}, r_{2t})\right\} \end{aligned}$$

or $|m_1\rangle = (e_{1t}, i_{1t}, r_{1t}) \overset{T_{1,0}}{\rightarrow} |n_1\rangle = (e_{1t}, i_{1t}, r_{1t})$ and $|m_2\rangle = (e_{2t}, i_{2t}, r_{2t}) \overset{T^+_{2,e_2^-}}{\rightarrow} |n_2\rangle = (e_{2t}-1, i_{2t}+1, r_{2t})$, with the corresponding probability:

$$\begin{aligned} &P\left(T_{1,0} \cap T^+_{2,e_2^-}\right) \\ &= P\left\{|n_1\rangle = (e_{1t}, i_{1t}, r_{1t}) \mid |m_1\rangle = (e_{1t}, i_{1t}, r_{1t}) \cap |n_2\rangle = (e_{2t}-1, i_{2t}+1, r_{2t}) \mid |m_2\rangle = (e_{2t}, i_{2t}, r_{2t})\right\}. \end{aligned}$$

This means that any increasing by one in random variable I during Δt requires only one of the two following events:

(i) an increasing by one, during Δt, in random variable I_1 during Δt, thus a decrement by one in the random variable E_1 during this time step;

(ii) an increasing by one, during Δt, in random variable I_2 during Δt, thus a decrement by one in the random variable E_2 or not during this time step.

Case (2): The transition T^- occurs if the two following transitions T^-_{1,r_1^+} and $T_{2,0}$ or two following transitions $T_{1,0}$ and $T^-_{2,0}$ or two following transitions $T_{1,0}$ and T^-_{2,r_2^+} are done simultaneously:

$$|m_1\rangle = (e_{1t}, i_{1t}, r_{1t}) \overset{T^-_{1,r_1^+}}{\rightarrow} |n_1\rangle = (e_{1t}, i_{1t}-1, r_{1t}+1) \text{ and } |m_2\rangle = (e_{2t}, i_{2t}, r_{2t}) \overset{T_{2,0}}{\rightarrow} |n_2\rangle = (e_{2t}, i_{2t}, r_{2t}),$$

with the corresponding probability:

$$\begin{aligned} &P\left(T^-_{1,r_1^+} \cap T_{2,0}\right) \\ &= P\left\{|n_1\rangle = (e_{1t}, i_{1t}-1, r_{1t}+1) \mid |m_1\rangle = (e_{1t}, i_{1t}, r_{1t}) \cap |n_2\rangle = (e_{2t}, i_{2t}, r_{2t}) \mid |m_2\rangle = (e_{2t}, i_{2t}, r_{2t})\right\} \end{aligned}$$

or $|m_1\rangle = (e_{1t}, i_{1t}, r_{1t}) \overset{T_{1,0}}{\rightarrow} |n_1\rangle = (e_{1t}, i_{1t}, r_{1t})$ and $|m_2\rangle = (e_{2t}, i_{2t}, r_{2t}) \overset{T^+_{2,0}}{\rightarrow} |n_2\rangle = (e_{2t}, i_{2t}+1, r_{2t})$, with the corresponding probability:

$$P\left(T_{1,0} \cap T^+_{2,0}\right) = P\left\{|n_1\rangle = (e_{1t}, i_{1t}, r_{1t}) \;\middle|\; |m_1\rangle = (e_{1t}, i_{1t}, r_{1t}) \cap |n_2\rangle = (e_{2t}, i_{2t}+1, r_{2t}) \;\middle|\; |m_2\rangle = (e_{2t}, i_{2t}, r_{2t})\right\}$$

or $|m_1\rangle = (e_{1t}, i_{1t}, r_{1t}) \overset{T_{1,0}}{\rightarrow} |n_1\rangle = (e_{1t}, i_{1t}, r_{1t})$ and $|m_2\rangle = (e_{2t}, i_{2t}, r_{2t}) \overset{T^-_{2,r_2^+}}{\rightarrow} |n_2\rangle = (e_{2t}, i_{2t}-1, r_{2t}+1)$, with the corresponding probability:

$$P\left(T_{1,0} \cap T^-_{2,r_2^+}\right) = P\left\{|n_1\rangle = (e_{1t}, i_{1t}, r_{1t}) \;\middle|\; |m_1\rangle = (e_{1t}, i_{1t}, r_{1t}) \cap |n_2\rangle = (e_{2t}, i_{2t}-1, r_{2t}+1) \;\middle|\; |m_2\rangle = (e_{2t}, i_{2t}, r_{2t})\right\}.$$

Then any decreasing by one, during Δt, in random variable I requires only one of the two following events:

(i) a decreasing by one, during Δt, in random variable I_1 during Δt, thus an increasing by one in the random variable R_1 during this time step;
(ii) a decreasing by one, during Δt, in random variable I_2 during Δt, thus an increasing by one in the random variable R_2 or not during this time step.

Case (3): The transition T happens if the two following transitions $T_{1,0}$ and $T_{2,0}$ or two following transitions T_{1,e_1^+} and $T_{2,0}$ or two following transitions T_{1,r_1^-} and $T_{2,0}$ or two following transitions $T_{1,0}$ and T_{2,e_2^+} or two following transitions $T_{1,0}$ and T_{2,e_2^-} or two following transitions $T_{1,0}$ and T_{2,r_2^-} are done simultaneously:

$$|m_1\rangle = (e_{1t}, i_{1t}, r_{1t}) \overset{T_{1,0}}{\rightarrow} |n_1\rangle = (e_{1t}, i_{1t}, r_{1t}) \text{ and } |m_2\rangle = (e_{2t}, i_{2t}, r_{2t}) \overset{T_{2,0}}{\rightarrow} |n_2\rangle = (e_{2t}, i_{2t}, r_{2t}),$$

with the corresponding probability:

$$P\left(T_{1,0} \cap T_{2,0}\right) = P\left\{|n_1\rangle = (e_{1t}, i_{1t}, r_{1t}) \;\middle|\; |m_1\rangle = (e_{1t}, i_{1t}, r_{1t}) \cap |n_2\rangle = (e_{2t}, i_{2t}, r_{2t}) \;\middle|\; |m_2\rangle = (e_{2t}, i_{2t}, r_{2t})\right\}$$

or $|m_1\rangle = (e_{1t}, i_{1t}, r_{1t}) \overset{T_{1,e_1^+}}{\rightarrow} |n_1\rangle = (e_{1t}+1, i_{1t}, r_{1t})$ and $|m_2\rangle = (e_{2t}, i_{2t}, r_{2t}) \overset{T_{2,0}}{\rightarrow} |n_2\rangle = (e_{2t}, i_{2t}, r_{2t})$, with the corresponding probability:

$$P\left(T_{1,e_1^+} \cap T_{2,0}\right) = P\left\{|n_1\rangle = (e_{1t}+1, i_{1t}, r_{1t}) \;\middle|\; |m_1\rangle = (e_{1t}, i_{1t}, r_{1t}) \cap |n_2\rangle = (e_{2t}, i_{2t}, r_{2t}) \;\middle|\; |m_2\rangle = (e_{2t}, i_{2t}, r_{2t})\right\}$$

or $|m_1\rangle = (e_{1t}, i_{1t}, r_{1t}) \overset{T_{1,r_1^-}}{\rightarrow} |n_1\rangle = (e_{1t}, i_{1t}, r_{1t}-1)$ and $|m_2\rangle = (e_{2t}, i_{2t}, r_{2t}) \overset{T_{2,0}}{\rightarrow} |n_2\rangle = (e_{2t}, i_{2t}, r_{2t})$, with the corresponding probability:

$$P\left(T_{1,r_1^-} \cap T_{2,0}\right) = P\left\{|n_1\rangle = (e_{1t}, i_{1t}, r_{1t}-1) \;\middle|\; |m_1\rangle = (e_{1t}, i_{1t}, r_{1t}) \cap |n_2\rangle = (e_{2t}, i_{2t}, r_{2t}) \;\middle|\; |m_2\rangle = (e_{2t}, i_{2t}, r_{2t})\right\}$$

or $|m_1\rangle = (e_{1t}, i_{1t}, r_{1t}) \overset{T_{1,0}}{\rightarrow} |n_1\rangle = (e_{1t}, i_{1t}, r_{1t})$ and $|m_2\rangle = (e_{2t}, i_{2t}, r_{2t}) \overset{T_{2,e_2^+}}{\rightarrow} |n_2\rangle = (e_{2t}+1, i_{2t}, r_{2t})$, with the corresponding probability:

$$P\left(T_{1,0} \cap T_{2,e_2^+}\right) = P\left\{|n_1\rangle = (e_{1t}, i_{1t}, r_{1t}) \;\middle|\; |m_1\rangle = (e_{1t}, i_{1t}, r_{1t}) \cap |n_2\rangle = (e_{2t}+1, i_{2t}, r_{2t}) \;\middle|\; |m_2\rangle = (e_{2t}, i_{2t}, r_{2t})\right\}$$

or $|m_1\rangle = (e_{1t}, i_{1t}, r_{1t}) \overset{T_{1,0}}{\rightarrow} |n_1\rangle = (e_{1t}, i_{1t}, r_{1t})$ and $|m_2\rangle = (e_{2t}, i_{2t}, r_{2t}) \overset{T_{2,e_2^-}}{\rightarrow} |n_2\rangle = (e_{2t}-1, i_{2t}, r_{2t})$, with the corresponding probability:

$$P\left(T_{1,0} \cap T_{2,e_2^-}\right) = P\left\{|n_1\rangle = (e_{1t}, i_{1t}, r_{1t}) \mid |m_1\rangle = (e_{1t}, i_{1t}, r_{1t}) \cap |n_2\rangle = (e_{2t}-1, i_{2t}, r_{2t}) \mid |m_2\rangle = (e_{2t}, i_{2t}, r_{2t})\right\}$$

or $|m_1\rangle = (e_{1t}, i_{1t}, r_{1t}) \overset{T_{1,0}}{\rightarrow} |n_1\rangle = (e_{1t}, i_{1t}, r_{1t})$ and $|m_2\rangle = (e_{2t}, i_{2t}, r_{2t}) \overset{T_{2,r_2^-}}{\rightarrow} |n_2\rangle = (e_{2t}, i_{2t}, r_{2t}-1)$, with the corresponding probability:

$$P\left(T_{1,0} \cap T_{2,r_2^-}\right) = P\left\{|n_1\rangle = (e_{1t}, i_{1t}, r_{1t}) \mid |m_1\rangle = (e_{1t}, i_{1t}, r_{1t}) \cap |n_2\rangle = (e_{2t}, i_{2t}, r_{2t}-1) \mid |m_2\rangle = (e_{2t}, i_{2t}, r_{2t})\right\}.$$

In this case, no change occurred in the random variable I during Δt, this requires only one of the three following events:

(i) no change in state, during Δt, for the four random variables I_1, I_2, E_1, E_2, R_1, and R_2";
(ii) no change in state, during Δt, for the two random variables I_1, I_2, with an increasing by one in the random variable E_1, or a decreasing by one in the random variable R_1 during this time step;
(iii) no change in state, during Δt, for the two random variables I_1,I_2, with an increasing by one in the random variable E_2, or a decreasing by one in the random variable E_2 or R_2, during this time step.

Case (4): A variety of multiple transitions, during Δt, with probability equal zero. All these above transitions can be summarized by defining the following two transitions: $|m_1\rangle = (e_{1t}, i_{1t}, r_{1t}) \overset{T_{|m_1\rangle,|n_1\rangle}}{\rightarrow} |n_1\rangle = (e'_{1t}, i'_{1t}, r'_{1t})$ and $|m_2\rangle = (e_{2t}, i_{2t}, r_{2t}) \overset{T_{|m_2\rangle,|n_2\rangle}}{\rightarrow} |n_2\rangle = (e'_{2t}, i'_{2t}, r'_{2t})$.

(B) Derivation of transition probabilities

To ensure that the transition probabilities given by system of equations (3.4) lie in the interval $[0, 1]$, the time step Δt must be chosen sufficiently small such that $\max(\sum_{j=1}^{11} P_j(\Delta t)) \leqslant 1$. $P_1(\Delta t) = P\left(T^+_{1,e_1^-} \cap T_{2,0}\right) = P\left(T^+_{1,e_1^-}|T_{2,0}\right) P(T_{2,0})$, where $P\left(T^+_{1,e_1^-}|T_{2,0}\right)$ is the conditional probability to have T^+_{1,e_1^-} given $T_{2,0}$. Since during the $T_{2,0}$ transition there is no change in the state of the random variables E_2, I_2, and R_2 then:

$$P\left(T^+_{1,e_1^-}|T_{2,0}\right) = P(T^+_{1,e_1^-}) = \alpha e_{1t}\Delta t,$$

where $\Theta(I_1, I_2) = \frac{k_1 I_1 + k_2 I_2}{k_1 N_1 + k_2 N_2}$, see reference [19]. We have

$$\sum_{|n_2\rangle} p_{|n_2\rangle,|m_2\rangle}(t+\Delta t, t) = 1 \iff$$

$$\begin{aligned}
&p_{(e_{2t},i_{2t},r_{2t}),(e_{2t},i_{2t},r_{2t})}(t+\Delta t, t) + p_{(e_{2t},i_{2t}+1,r_{2t}),(e_{2t},i_{2t},r_{2t})}(t+\Delta t, t) + p_{(e_{2t}-1,i_{2t}+1,r_{2t}),(e_{2t},i_{2t},r_{2t})}(t+\Delta t, t)\\
&\quad + p_{(e_{2t},i_{2t}-1,r_{2t}),(e_{2t},i_{2t},r_{2t})}(t+\Delta t, t) + p_{(e_{2t},i_{2t}-1,r_{2t}+1),(e_{2t},i_{2t},r_{2t})}(t+\Delta t, t)\\
&\quad + p_{(e_{2t}+1,i_{2t},r_{2t}),(e_{2t},i_{2t},r_{2t})}(t+\Delta t, t) + p_{(e_{2t}-1,i_{2t},r_{2t}),(e_{2t},i_{2t},r_{2t})}(t+\Delta t, t)\\
&\quad + p_{(e_{2t},i_{2t},r_{2t}-1),(e_{2t},i_{2t},r_{2t})}(t+\Delta t, t) = 1,
\end{aligned}$$

by adopting the simple notations we write:

$$P(T_{2,0}) = 1 - P\left(T^+_{2,0}\right) - P\left(T^+_{2,e_2^-}\right) - P\left(T^-_{2,0}\right) - P\left(T^-_{2,r_2^+}\right) - P\left(T_{2,e_2^+}\right) - P\left(T_{2,e_2^-}\right) - P\left(T_{2,r_2^-}\right),$$

where

$$P\left(T^{+}_{2,0}\right)=\eta_2 N_2,\qquad P\left(T^{+}_{2,e_2^-}\right)=\alpha e_{2t}\Delta t,\qquad P\left(T^{-}_{2,0}\right)=\mu i_{2t}\Delta t,$$
$$P\left(T^{-}_{2,r_2^+}\right)=\gamma i_{2t}\Delta t,\qquad P\left(T_{2,e_2^+}\right)=\beta k_2\Theta\left(i_{1t},i_{2t}\right)\left(N_2-e_{2t}-i_{2t}-r_{2t}\right)\Delta t,\qquad P\left(T_{2,e_2^-}\right)=\mu e_{2t}\Delta t,$$
$$P\left(T_{2,r_2^-}\right)=\mu r_{2t}\Delta t.$$

Hence,

$$P\left(T_{2,0}\right)=1-\left[\eta_2 N_2+\alpha e_{2t}+\beta k_2\Theta\left(i_{1t},i_{2t}\right)\left(N_2-e_{2t}-i_{2t}-r_{2t}\right)+\mu\left(e_{2t}+r_{2t}\right)+\left(\mu+\gamma\right)i_{2t}\right]\Delta t.$$

We finally obtain:

$$P_1\left(\Delta t\right)=\alpha e_{1t}\Delta t\left\{1-\left[\eta_2 N_2+\alpha e_{2t}+\beta k_2\Theta\left(i_{1t},i_{2t}\right)\left(N_2-e_{2t}-i_{2t}-r_{2t}\right)+\mu\left(e_{2t}+r_{2t}\right)+\left(\mu+\gamma\right)i_{2t}\right]\Delta t\right\}.$$

With the same analysis, we also calculate other transition possibilities:

$$\begin{aligned}
P_2\left(\Delta t\right)&=\left\{1-\left[\delta r_{1t}+\beta k_1\Theta\left(i_{1t},i_{2t}+1\right)\left(N_1-e_{1t}-i_{1t}-r_{1t}\right)+\alpha e_{1t}+\gamma i_{1t}\right]\Delta t\right\}\mu_2 N_2\Delta t,\\
P_3\left(\Delta t\right)&=\left\{1-\left[\delta r_{1t}+\beta k_1\Theta\left(i_{1t},i_{2t}+1\right)\left(N_1-e_{1t}-i_{1t}-r_{1t}\right)+\alpha e_{1t}+\gamma i_{1t}\right]\Delta t\right\}\alpha e_{2t}\Delta t,\\
P_4\left(\Delta t\right)&=\gamma i_{1t}\Delta t\left\{1-\left[\eta_2 N_2+\alpha e_{2t}+\beta k_2\Theta\left(i_{1t},i_{2t}\right)\left(N_2-e_{2t}-i_{2t}-r_{2t}\right)+\mu\left(e_{2t}+r_{2t}\right)+\left(\mu+\gamma\right)i_{2t}\right]\Delta t\right\},\\
P_5\left(\Delta t\right)&=\left\{1-\left[\delta r_{1t}+\beta k_1\Theta\left(i_{1t},i_{2t}-1\right)\left(N_1-e_{1t}-i_{1t}-r_{1t}\right)+\alpha e_{1t}+\gamma i_{1t}\right]\Delta t\right\}\gamma i_{2t}\Delta t,\\
P_6\left(\Delta t\right)&=\left\{1-\left[\delta r_{1t}+\beta k_1\Theta\left(i_{1t},i_{2t}+1\right)\left(N_1-e_{1t}-i_{1t}-r_{1t}\right)+\alpha e_{1t}+\gamma i_{1t}\right]\Delta t\right\}\mu i_{2t}\Delta t,\\
P_7\left(\Delta t\right)&=\left\{1-\left[\delta r_{1t}+\beta k_1\Theta\left(i_{1t},i_{2t}+1\right)\left(N_1-e_{1t}-i_{1t}-r_{1t}\right)+\alpha e_{1t}+\gamma i_{1t}\right]\Delta t\right\}\mu r_{2t}\Delta t,\\
P_8\left(\Delta t\right)&=\beta k_1\Theta\left(i_{1t},i_{2t}\right)\left(N_1-e_{1t}-i_{1t}-r_{1t}\right)\Delta t\left\{1-\left[\delta r_{1t}+\beta k_1\Theta\left(i_{1t},i_{2t}+1\right)\right.\right.\\
&\quad\left.\left.\times\left(N_1-e_{1t}-i_{1t}-r_{1t}\right)+\alpha e_{1t}+\gamma i_{1t}\right]\Delta t\right\},\\
P_9\left(\Delta t\right)&=\delta r_{1t}\Delta t\left\{1-\left[\delta r_{1t}+\beta k_1\Theta\left(i_{1t},i_{2t}+1\right)\left(N_1-e_{1t}-i_{1t}-r_{1t}\right)+\alpha e_{1t}+\gamma i_{1t}\right]\Delta t\right\},\\
P_{10}\left(\Delta t\right)&=\left\{1-\left[\delta r_{1t}+\beta k_1\Theta\left(i_{1t},i_{2t}\right)\left(N_1-e_{1t}-i_{1t}-r_{1t}\right)+\alpha e_{1t}+\gamma i_{1t}\right]\Delta t\right\}\beta k_2\Theta\left(i_{1t},i_{2t}\right)\\
&\quad\times\left(N_2-e_{2t}-i_{2t}-r_{2t}\right)\Delta t,\\
P_{11}\left(\Delta t\right)&=\left\{1-\left[\delta r_{1t}+\beta k_1\Theta\left(i_{1t},i_{2t}\right)\left(N_1-e_{1t}-i_{1t}-r_{1t}\right)+\alpha e_{1t}+\gamma i_{1t}\right]\Delta t\right\}\mu e_{2t}\Delta t.
\end{aligned}$$

Since

$$\sum_{j=1}^{12}P_j\left(\Delta t\right)=1,$$

then

$$P_{12}\left(\Delta t\right)=1-\sum_{j=1}^{11}P_j\left(\Delta t\right).$$

References

[1] D. Acarali, M. Rajarajan, N. Komninos, B. B. Zarpelao, *Modelling the spread of botnet malware in IoT-based wireless sensor networks*, Secur. Commun. Netw., **2019** (2019), 13 pages. 1

[2] L. J. S. Allen, *An introduction to stochastic processes with applications to biology*, CRC Press, Boca Raton, FL, (2011). 2

[3] L. J. S. Allen, *An introduction to stochastic epidemic models*, In: Mathematical epidemiology, Springer, Berlin, **1945** (2008), 81–130.

[4] L. J. S. Allen, E. J. Allen, *A comparison of three different stochastic population models with regard to persistence time*, Theor. Popul. Biol., **64** (2003), 439–449. 2

[5] J. Amador, *The stochastic SIRA model for computer viruses*, Appl. Math. Comput., **232** (2014), 1112–1124. 2

[6] A.-L. Barabási, R. Albert, *Emergence of scaling in random networks*, Science, **286** (1999), 509–512. 1

[7] A.-L. Barabási, R. Albert, H. Jeong, *Mean-field theory for scale-free random networks*, Phys. A, **272** (1999), 173–187. 1

[8] P. Buesser, F. Daolio, M. Tomassini, *Optimizing the robustness of scale-free networks with simulated annealing*, In: Adaptive and Natural Computing Algorithms: 10th International Conference, ICANNGA 2011, Ljubljana, Slovenia, April 14-16, 2011, Proceedings, Part II 10., Springer, Berlin Heidelberg, (2011), 167–176 1

[9] P. De, Y. Liu, S. K. Das, *Modeling node compromise spread in wireless sensor networks using epidemic theory*, In: 2006 International Symposium on a World of Wireless, Mobile and Multimedia Networks(WoWMoM'06), IEEE, (2006), 7 pages. 1

[10] Y. Duan, X. Fu, W. Li, Y. Zhang, G. Fortino, *Evolution of scalefree wireless sensor networks with feature of small-world networks*, Complexity, **2017** (2017), 15 pages. 1

[11] Y. El Ansari, T. Chaayra, F. El Bouanani, L. Omari, M. Amrouch, *Strong consistency estimators of the Brennan-Schwartz diffusion process based on martingales approach*, Stat, **11** (2022), 20 pages. 3.2

[12] Y. El Ansari, A. El Myr, L. Omari, *Deterministic and stochastic study for an infected computer network model powered by a system of antivirus programs*, Discrete Dyn. Nat. Soc., **2017** (2017), 13 pages. 2

[13] Y. El Ansari, A. El Myr, L. Omari, A. Lahrouz, *The effect of immigration on the persistence and ergodicity of a stochastic SIS model for transmission of disease*, Appl. Math. Inf. Sci., **12** (2018), 1127–1138. 3.2

[14] M. Essouifi, A. Achahbar, *A mixed sir-sis model to contain a virus spreading through networks with two degrees*, Int. J. Mod. Phys. C, **28** (2017), 19 pages. 1, 2, 3.1

[15] M. Essouifi, A. Achahbar, *Discrete stochastic modelling of computer viruses prevalence on a reduced scale-free network*, Int. J. Comput. Appl. Technol., **63** (2020), 257–271. 2, 3.1

[16] H. J. Herrmann, C. M. Schneider, A. A. Moreira, J. S. Andrade Jr, S. Havlin, *Onion-like network topology enhances robustness against malicious attacks*, J. Stat. Mech., **2011** (2011). 1

[17] Y. Jian, E. Liu, Y. Wang, Z. Zhang, C. Lin, *Scale-free model for wireless sensor networks*, In: 2013 IEEE Wireless Communications and Networking Conference (WCNC), IEEE, (2013), 2329–2332 1

[18] L. Jiang, X. Jin, Y. Xia, B. Ouyang, D. Wu, X. Chen, *A scale-free topology construction model for wireless sensor networks*, Int. J. Distrib. Sens. Netw., **2014** (2014), 8 pages. 1

[19] N. Keshri, A. Gupta, B. K. Mishra, *Impact of reduced scale free network on wireless sensor network*, Phys. A, **463** (2016), 236–245. (document), 1, 2, 3.1, 4.1, 5

[20] G. Liu, Z. Tan, Z. Liang, H. Chen, X. Zhong, *Fractional optimal control for malware propagation in the internet of underwater things*, IEEE Internet Things J., **11** (2024), 11632–11651. 1

[21] B. K. Mishra, N. Keshri, *Mathematical model on the transmission of worms in wireless sensor network*, Appl. Math. Model., **37** (2013), 4103–4111. 1

[22] B. K. Mishra, S. K. Srivastava, B. K. Mishra, *A quarantine model on the spreading behavior of worms in wireless sensor network*, Trans. IoT. Cloud Comput., **2** (2014), 1–12.

[23] B. K. Mishra, I. Tyagi, *Defending against malicious threats in wireless sensor network: A mathematical model*, Int. J. Inf. Technol. Comput. Sci., **6** (2014), 12–19. 1

[24] S. Muthukrishnan, S. Muthukumar, V. Chinnadurai, *Optimal control of malware spreading model with tracing and patching in wireless sensor networks*, Wirel. Pers. Commun., **117** (2021), 2061–2083. 1, 2

[25] I. Nåsell, *Stochastic models of some endemic infections*, Math. Biosci., **179** (2002), 1–19. 2

[26] D. M. Nicol, *The impact of stochastic variance on worm propagation and detection*, In: Proceedings of the 4th ACM workshop on Recurring malcode, (2006), 57–64. 2

[27] K. S. Nisar, Y. Sabbar, *Long-run analysis of a perturbed HIV/AIDS model with antiretroviral therapy and heavy-tailed increments performed by tempered stable Lévy jumps*, Alex. Eng. J., **78** (2023), 498–516. 3.2

[28] C. H. Nwokoye, V. Madhusudanan, M. N. Srinivas, N. N. Mbeledogu, *Modeling time delay, external noise and multiple malware infections in wireless sensor networks*, Egypt. Inform. J., **23** (2022), 303–314. 2

[29] M. Ochab, P. Manfredi, K. Puszynski, A. d'Onofrio, *Multiple epidemic waves as the outcome of stochastic sir epidemics with behavioral responses: a hybrid modeling approach*, Nonlinear Dyn., **111** (2023), 887–926. 2

[30] R. P. Ojha, P. K. Srivastava, G. Sanyal, N. Gupta, *Improved model for the stability analysis of wireless sensor network against malware attacks*, Wirel. Pers. Commun., **116** (2021), 2525–2548. 1

[31] T. Qiu, A. Zhao, F. Xia, W. Si, D. O. Wu, *Rose: Robustness strategy for scale-free wireless sensor networks*, IEEE/ACM Trans. Netw., **25** (2017), 2944–2959. 1

[32] A. Rey, J. Guillén, G. R. Sánchez, *Modeling malware propagation in wireless sensor networks with individual-based models*, In: Conference of the Spanish Association for Artificial Intelligence, Springer, Cham, **9868** (2016), 194–203. 1

[33] K. R. Rohloff, T. Bacşar, *Deterministic and stochastic models for the detection of random constant scanning worms*, ACM Trans. Model. Comput. Simul., **18** (2008), 1–24. 2

[34] P. K. Roy, J. Mondal, R. Bhattacharyya, S. Bhattacharya, T. Szabados, *Extinction of disease pathogenesis in infected population and its subsequent recovery: a stochastic approach*, J. Appl. Math., **2013** (2013), 8 pages. 2

[35] Y. Sabbar, A. Din, D. Kiouach, *Influence of fractal–fractional differentiation and independent quadratic Lévy jumps on the dynamics of a general epidemic model with vaccination strategy*, Chaos Solitons Fractals, **171** (2023). 3.2

[36] Y. Sabbar, J. L. D. Palencia, M. Tilioua, A. Otero, A. Zeb, S. Djilali, *A general chemostat model with second-order Poisson jumps: asymptotic properties and application to industrial waste-water treatment*, AIMS Math., **8** (2023), 13024–13049.

[37] Y. Sabbar, M. Yavuz, F. Özköse, *Infection Eradication Criterion in a General Epidemic Model with Logistic Growth, Quarantine Strategy, Media Intrusion, and Quadratic Perturbation*, Mathematics, **10** (2022), 16 pages. 3.2

[38] F. D. Sahneh, C. Scoglio, P. Van Mieghem, *Generalized epidemic mean-field model for spreading processes over multilayer complex networks*, IEEE/ACM Trans. Netw., **21** (2013), 1609–1620. 2

[39] F. D. Sahneh, A. Vajdi, H. Shakeri, F. Fan, C. Scoglio, *Gemfsim: A stochastic simulator for the generalized epidemic modeling framework*, J. Comput. Sci., **22** (2017), 36–44. 2

[40] S. Shen, H. Zhou, S. Feng, J. Liu, Q. Cao, *SNIRD: Disclosing rules of malware spread in heterogeneous wireless sensor networks*, IEEE Access, **7** (2019), 92881–92892. 1

[41] S. Shen, H. Zhou, S. Feng, J. Liu, H. Zhang, Q. Cao, *An epidemiology-based model for disclosing dynamics of malware propagation in heterogeneous and mobile wsns*, IEEE Access, **8** (2020), 43876–43887.

[42] A. Singh, A. K. Awasthi, K. Singh, P. K. Srivastava, *Modeling and analysis of worm propagation in wireless sensor networks*, Wirel. Pers. Commun., **98** (2018), 2535–2551. 1

[43] J. H. Steele, *A comparison of terrestrial and marine ecological systems*, Nature , **313** (1985), 355–358. 3.2

[44] L. Wang, J. Dang, Y. Jin, H. Jin, *Scale-free topology for largescale wireless sensor networks*, In: 2007 3rd IEEE/IFIP International Conference in Central Asia on Internet, IEEE, (2007), 1–5. 1

[45] Y. Yang, G. Liu, Z. Liang, H. Chen, L. Zhu, X. Zhong, *Hybrid control for malware propagation in rechargeable WUSN and WASN: from knowledge-driven to data-driven*, Chaos Solitons Fractals, **173** (2023), 20 pages. 1

[46] L.-X. Yang, X. Yang, *The spread of computer viruses over a reduced scale-free network*, Phys. A, **396** (2014), 173–184. 1, 2

[47] X. Ye, W. Zhuo, *A scale-free routing algorithm in wireless sensor networks*, In: 2008 Second International Conference on Future Generation Communication and Networking, IEEE, **1** (2008), 465–468. 1

[48] X. Zhang, *Model design of wireless sensor network based on scalefree network theory*, In: 2009 5th International Conference on Wireless Communications, Networking and Mobile Computing, IEEE, (2009), 1–4. 1

[49] C. Zhang, Y. Zhao, Y. Wu, S. Deng, *A stochastic dynamic model of computer viruses*, Discrete Dyn. Nat. Soc., **2012** (2012), 16 pages. 3.2

[50] H. Zhang, V. Madhusudanan, R. Geetha, M. N. Srinivas, C. H. Nwokoye, *Dynamic analysis of the e-sitr model for remote wireless sensor networks with noise and sokol-howell functional response*, Results Phys., **38** (2022). 2

[51] X. Zhong, B. Peng, F. Deng, G. Liu, *Stochastic stabilization of malware propagation in wireless sensor network via aperiodically intermittent white noise*, Complexity, **2020** (2020), 13 pages. 2